STUDIES ON THE STRESS – STRAIN PROPERTIES OF CORDS FOR FISHING GEAR MATERIALS

By

Bambang MURDIYANTO

Faculty of Fisheries, Hokkaido University

Contents

1. Introduction

Finn, B., Director of the Fisheries Division, F.A.O., has declared that the progress in the fisheries has been greater in the past 50 years and that the advent of synthetic fibres was the third of the main technological revolutions in the modern fishing development[1]. The first revolution was the mechanization and the second revolution to influence modern fishing was the use of electronic echo sounding and echo ranging equipment.

Nylon in various forms was the first of the man made fibres to be widely applied in fishing nets, but in recent years, several other synthethic have also become important especially in Japan, which leads the world in using synthetic fibres for fishing, both in regards to quantity and variety. The properties of synthetic fibers such as high tenacity and relatively low extensibility or lower tensile strength and high extensibility are important factors when selecting synthetic fibers for fishing. To keep pace with development, scientific and application research is essential, the more we known about the properties of the various fibers, the better we shall be able to employ them in the most useful and appropriate way[2].

Studies on the properties of synthetic fibres have been done for many years. The geometrical structure of multiply yarn have been studied theoretically by Treloar, L.R.G.[3], Gracie, P.S.[4], Freeston, W.D., and M.M. Schoppee[5] and Riding, G.[6] and studied experimentally by Tattersal, G.H.[7], Riding, G.[8] and Iyer, K.B.[9]. Hearle, J.W.S. and O.N. Bose[10] studied the form of yarn twisting. Studies on the tensile properties of continuous filament yarn have been done by Hearle[11], Treloar and Riding[12], Kilby, W.F.[13] and Platt, M.M.[14]. Treloar and Riding have developed a theory to consider the problem of the interpretation of the tensile properties of twisted continuous filament yarn in term of their geometrical structure and the strain-energy of the system. Kilby's paper deals essentially with certain theoretical aspects of the mechanical properties of twisted continuous filament yarn, particularly the effect of the equalization of filament tensions on initial modulus, tenacity, and breaking extension. Platt, derived mathematical formulas to express variations in tensile characteristics, both for one-time loading to rupture and repeated stress as a function of yarn geometry.

Fishing gear, net and cord, in its used for fish catching, will be subjected to various deformations on tensioning, impact stretching, loading, abrassive action etc. that influence the utility and resisting-power of the gear. Studies to improve fishing gear construction and efficiency can be approached in many different ways and great possibilities to improve fishing gear and methods still exist. It is logical not only to study the fishing gear to improve its construction and efficiency but also to study the materials from which the gear is made. It is important to determine the properties of materials, including geometrical structures, tensile strength and the stress-strain diagram. In particular, the man made fibres will continue to be invented and will continually become available for making nets. To fulfil the desired properties for getting better constructed and more efficient fishing gear, studies on the stress-strain properties of materials are of great importance. As a result of these studies, fishing gear will be designed and constructed on a more rational basis and the fishing effort will become more effective.

The studies on the stress-strain properties of multiply cords have been studied theoretically by Treloar[15] and experimentally by Riding[16]. In those studies the strainenergy method that was previously used to derive the stress-strain curve of twisted continuous filament yarn by the same authors is applied to the derivation of the corresponding properties of continuous filament cords of two-ply, three-ply and seven-ply constructions.

In Japan, in the field of fisheries, the properties of materials for fishing have

been studied a long time in the past 50 years. Tauti, M.[17] studied the strength of cord in relation to the twist employing cotton and ramie, materials made from natural fibres, as the experimental materials. Koizumi, T.[18),19),20] studied the tensile strength of synthetic netting materials of various twist. Honda, K. and S. Osada[21] studied the experimental tests on polypropylene twine to ascertain their properties in relation to other synthetic materials. Shimozaki, Y. and H. Kato[22] studied the continuous filament twines on their wear resistance. Sato, O. et al.[23] made a study on the change of the breaking tensile strength of thread on monofilament. Studies involving the problem of stress-strain properties of materials have been carried out by Yamamoto, K.[24] in his studies about the geometrical structure of materials used for fishing nets and the mechanical properties of materials.

The work of Treloar[15] is the applciation of theoretical calculation to the cords constructed to the so called 'single yarn' describe as a large number of filaments twisted together. What is called the 'cord' by Treloar is the construction by twisting 2, 3 or more plies of single yarns. Differently, in this study, the theory should be applied to the cord constructed of 'monofilament yarns'. Such products are widely used as netting materials. And a cord or twine made by twisting several threads of monofilament yarns are usually called 'plied monofilament' or 'folded monofilament yarn'. The application of Treloar's theory for the construction of plied monofilament yarn netting material seems not to be applicable. From this consideration studies on the stress-strain properties of netting materials constructed as plied monofilament yarn are necessary. For this purpose, beginning with the twisted single monofilament yarn, simple plied monofilament yarns of 2-ply and 3-ply construction to the more complex model of multiplied monfilament yarns are studied. Such a study at the present time has not been found.

The purpose of this study is first, to make an attempt to determine a basis for the prediction of the stress-strain curve of a twisted monofilament yarn up near to the breaking point from the stress-strain curve of initial monofilament yarn. The basic assumptions and the geometrical calculation of strain adopted in this study are similar to those developed by Treloar[11], but the stresses are calculated in usual method in term of the ratio of the force to the mass/unit length. Despite the similarity of the theory developed by Treloar and the theory used in this study, the conception of 'neutral zone layer' is introduced in this study. The calculation of stress and strain for a twisted monofilament yarn are carried out refering to the neutral zone layer.

Secondly, based on the theory developed for calculating the twisted monofilament yarn stress-strain curve, the same general method is developed and applied to the more complex problem of two-ply and three-ply cords constructed from monofilament yarn. Theory and experimental verification are made for two kinds of cord construction. One is of two-ply and three-ply cord single-yarn strand, the other is of two-ply and three-ply cord multiply-yarn strand.

The main theoretical aspects are described in chapter 2. Chapter 3 contains the experimental procedure, experimental materials and methods for the verification to the theory developed previously. Chapter 4 is describing the comparison

between calculated and experimental values and its supplement calculation methods for obtaining the calculated values. General discussion and conclusions about the experimental results, its comparison with the calculated values and any disagreement between theory and experiments are made in the last chapters. It is concluded that the theoretical calculation can predict well the experimental curve, and that from the known initial yarn curve the desired form of stress-strain curve within a reasonable range of a cord may be designed and constructed.

Before going further, the author acknowledges his indebtedness to Prof. Dr. O. Sato, Prof. Dr. S. Igarashi, Associate Prof. Dr. K. Nashimoto and Dr. K. Yamamoto of the Faculty of Fisheries, Hokkaido University, for their continuous interest through this study. Much appreciation is also due to Mr. Y. Hiranaga, Deputy Director of Hakodate Fish-net and Ships Manufacturing Co. and his staff members, Mr. M. Nakazawa and the staff members of the Research and Development section of this company for their kind help and assistance in the sample preparation and material supply. Finally many thanks to Miss. C. Nakayama, the secretary of the Laboratory of Fishing Gear Engineering of this Faculty and the post graduate students in this Laboratory for their kind help in the preparation of this paper.

2. Theoretical aspects

2.1 Terminology and principal symbols used

The terminology used to describe yarn, twine or cord constructions have been written in many ways such as in British Standard Institution for textile industry[25], and others in fisheries field. Nevertheless the technical terms as well as numbering systems differ from country to country and between different field of study. Heyhurst, G.A. and A. Robinson[26] speaking from the twine maker's point of view about the construction of twines and strands, and Stutz, H.[27] gave the classification of all kinds of fibres and pointed out the difficulties of using the different kinds of fibre numbering system as well as different units of measurement. Takayama, S.[28] who gave the terminology and numbering system used in Japan, gave these general denotations of threads, twines, ropes and cords in this following formula.

Fibre			
〃	Yarn		
〃	〃	Strand	Thread
	〃	〃	Twine
		〃	Rope

Klust, G.[29] reviewed the terminology used for fishing industry based on the recommendations of the International Organization for Standardization (ISO) which among other things suggested that the term 'strand' and 'cord' should not be used in fisheries, but Robinson, A.[30] emphasized that the term 'strand' was well known because of its use in ropes where it was the standard term and that if the term was abandoned, it could leave some difficulties in describing the twine

construction. According to the terminology described by Klust, if several threads of monofilament yarns are twisted together, the term 'folded monofilament yarn' or 'plied monofilament yarn' should be used.

In this study, although that the construction of the samples prepared should be mentioned as 'plied monofilament yarn' or 'folded monofilament yarn' if referring to the above definitions, for the purpose of getting better acquainted to the problem involving the theory and its experimental verifications, other terms were used. The terms for the constructions of samples used for experimental were determined as follows.

One thread of monofilament when it is twisted is called 'twisted monofilament'. Several of twisted monofilament yarns if twisted together resulted a 'strand' and when several 'strands' are twisted together, the final product will be called a 'cord'. But a strand construction may be the final product, in this case the final product should be called a 'cord'. To distinguish between a 'cord' resulting from the strand construction as a final result and a 'cord' made by twisting several strands, the terms 'cord single yarn strand' and 'cord multiply-yarn strand' are used respectively. Then, in this study, we have the term 'two-ply cord single-yarn strand' to describe a cord consisting of two strands in which each strand consist of only one thread of monofilament yarn (see Fig. 2.1). The term 'three ply cord single-yarn strand' is describing a cord consisting of three strands in which each strand consists of one thread of monofilament yarn. Fig. 2.2 describ the cords constructed from multiply-yarn strands which are defined as follows. 'Two ply cord multiply-yarn strand' is used to describe a cord having 2-ply strands in which each strand consist of 2–, 3–, 7–, or 19– ply of monofilament yarn, so that as an example, 2–ply cord 7–yarn strand is a cord of 2 strands in which each strand consist of 7–ply of monofilament yarns. The term '3–ply cord multiply-yarn strand' is used to describe a cord consisting of 3 strands as its plies, in which each strand consist of 2–ply, 3–ply, 7–ply and 19–ply yarns, so that '3–ply cord 3–yarn strand' is a cord consisting of 3 strands in which each strand consist of 3–ply of monofilament yarns. '3–ply cord 19–yarn strand' is a cord consisting of 3 strands in which each strand consist of 19–ply monofilament yarns (see Fig. 2.2 as an example of a cord of multiply-yarn strand). The notations used

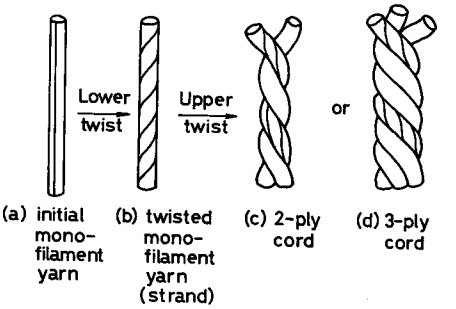

Fig. 2.1. Constructions of 2-play and 3-ply cord single yarn strand.

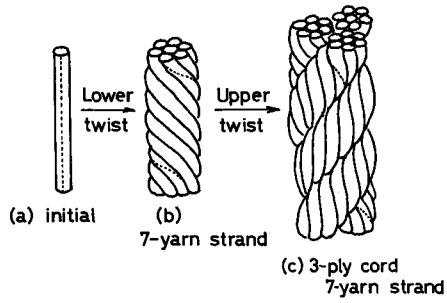

Fig. 2.2 Construction of 3-ply cord 7-yarn strand.

to describe the construction of cords are given as follows.
2/4 for 2-ply cord 2-yarn strand,
2/14 for 2–ply cord 7–yarn strand,
3/6 for 3–ply cord 2–yarn strand,
3/9 for 3–ply cord 3–yarn strand,
3/57 for 3–ply cord 19–yarn strand, etc.

In describing the geometry and its change in the cord as well as in the ply, strand or initial monofilament yarn the following symbols are used.

On the twisted monofilament

Items	initial	twisted	twisted and strained
Monofilament yarn length for one turn	h_i	h_0	h_t
Fibril length	l_i	$l_{0(\theta)}$	$l_{t(\theta)}$
Radius of monofilament yarn	R_i	R_0	R_t
Radial position of cylindrical layer	r_i	r_0	r_t
Thickness of cylindrical layer	dr_i	dr_0	dr_t
Radial position of neutral zone layer	—	a_0	a_t
Monofilament yarn extension ratio	—	—	λ_t
Stress in the twisted monofilament	—	—	σ_t

Notes: (θ) is the fibril helix angle to the yarn axis,
(α) refer to the fibril at neutral zone layer
(β) refer to the fibril at yarn surface

On the 2-ply and 3-ply cords single yarn strand

Items	unstrained state	strained state
Cord diameter	d_0	d_t
Cord helix angle	γ_0	γ_t

Cord helix radius	c_0	c_t
Cord surface helix angle	φ_0	φ_t
Cord twist (in turns per unit length)	N_0	N_t
Cord torsion	τ_{co}	τ_{ct}
Cord extension ratio	—	λ_c
Stress in the cord	—	σ_c
Ply (strand) diameter	b_0	b_t
Ply axis length	p_0	p_t
Ply twist (in turns per unit length)	n_0	n_t
Ply torsion	τ_0	τ_t
Ply extension ratio	—	λ_t
Stress in the ply	—	σ_t

On the 2-ply and 3-ply cords multiply-yarns strand

Items	unstrained state	strained state
Cord diameter	d_0	d_t
Cord helix angle	γ_0	γ_t
Cord helix radius	c_0	c_t
Cord axial length	m_0	m_t
Cord twist	N_0	N_t
Cord surface helix angle	φ_0	φ_t
Cord torsion	τ_{co}	τ_{ct}
Cord extension ratio	—	λ_c
Stress in the cord	—	σ_c
Ply (strand) diameter	b_0	b_t
Strand axial length	p_0	p_t
Strand twist	n_0	n_t
Strand torsion	τ_0	τ_t
Strand helix angle (outer monofilament yarn axis helix angle)	δ_0	δ_t
Strand helix radius (outer monofilament yarn axis helix radius)	c_0'	c_t'
Monofilament yarn torsion (as ply in the strand)	τ_0'	τ_t'
Strand extension ratio	—	λ_p
Stress in the strand	—	σ_p

2.2 Basic assumptions

It is necessary for the basic assumptions to be adopted in order to be able to develop theoretical calculations. In this study it is assumed that the twisted monofilament can be considered as the twisted yarn in which the fibirls are regarded as filaments in the yarn held together by cohesive force. Then it might be further assumed that

1. The monofilament yarn has a circular cross section which does not change after

the monofilament is twisted, and that the volume of the monofilament yarn remain constant throughout twisting and tensioning.
2. The fibrils in the monofilament yarn possess uniform properties along their length, and all the fibril properties are regarded as being identical.
3. The fibrils form a helicocylindrical structure without any fibril migration in the twisted monofilament.
4. The fibrils at the neutral zone layer have the same stress-strain properties as the initial monofilament yarn stress-strain properties.
5. The Young's modulus of the fibril is constant throughout tensioning and compressioning.
6. In the cords of single-yarn strand the fibrils in the plies form a 'doubly wound helix', so that each ply is composed of a set of co-axial helices wound about a single helical axis. In the cord of multiply-yarns strand, each ply is composed of a set of co-axial helices of yarns wound about a single helical axis.
7. Each strand (ply in the cord) and each monofilament yarn as the ply in the strand, which has an axis that formed a helix wound around the cord axis or the strand axis, have the stress-strain properties which are the same as if the strand and the monofilament yarn axis are in the straight condition.
8. Each ply in the cord has a circular cross section which will not change its shape during tensioning.

2.3 On the twisted monofilament yarn

2.3.1 The neutral zone layer

The monofilament yarn can be considered as a long rod with circular cross section. In this rod a cylindrical layer is distinguished with an inner initial radius r_i, a thickness dr_i and a length h_i. The layer consists of fibrils which are parallel to the rod axis. After some turns of twisting are given to the rod, its length decreases to h_0 and the fibril at any radius r_i from the monofilament yarn axis will move innerward and its radius from the yarn axis become r_0 and the fibril would form a helix with an angle θ toward the monofilament yarn axis. The thickness of the cylindrical layer become dr_0.

Zurek, W.[31] has found that in the twisted monofilament the stresses in the outer zone result in a compression of the inner zone. According to that statement it must be considered that there is a compressional zone in the inner part where the fibrils length decrease and a tensional zone in the outer part where the fibrils length extend to some strain. There is a layer between the compressional and tensional zone where the fibrils length remain constant before and after twisting, and this layer will be called the neutral zone layer. The geometry of this neutral zone layer and the theory to calculate the stress-strain curve of twisted monofilament yarn derived from the known initial monofilament yarn stress-strain curve has been developed by Murdiyanto, B. and O. Sato in a previous study[32].

Since in this present study a more complex problem of cords constructions is involved, different symbols and subscripts are used, and it is necessary to represent here the important formula developed in the previous study[32] by using

the new symbols. Some corrections have also been made here.

It has been obtained that by assuming that the Young's modulus of the fibrils are constant, the helix angle of the fibril at the neutral zone layer can be written as[32],

$$\sec \alpha_0 = \frac{\sec \beta_0 - 1}{ln \sec \beta_0} \tag{2-1}$$

where α_0 is the helix angle of the fibril at the neutral zone layer, and β_0 is the helix angle of the fibril at the monofilament yarn surface.

2.3.2 Geometry of strain and stress.

If any tensional force is given to the twisted monofilament yarn, the fibril length will extend with the extension ratio of $\lambda_{(\theta t)}$ and can be written as,

$$\lambda_{(\theta t)} = \frac{l_{t(\theta)}}{l_{0(\alpha)}}, \tag{2-2}$$

and the twisted monofilament yarn itself will extend with the extension ratio of λ_t written as

$$\lambda_t = \frac{h_t}{h_0} \tag{2-3}$$

At the neutral zone layer the fibril will extend at the same extension ratio of the initial monofilament yarn extension ratio, written as

$$\frac{l_{t(\alpha)}}{l_{0(\alpha)}} = \frac{l_{it}}{l_i} = \frac{h_{it}}{h_i} = \lambda_i \tag{2-4}$$

where l_{it} is the length of the fibril in the untwisted monofilament yarn after strained, and h_{it} is the length of the untwisted monofilament yarn in the strained condition.

The relation of the initial monofilament yarn extension ratio, λ_i, and the twisted monofilament yarn extension ratio, λ_t, were obtained in the previous study[32] as

$$\lambda_i^2 = \frac{\lambda_t^2(1+\lambda_t^{-3}\tan^2\alpha_0)}{\sec^2\alpha_0} \tag{2-5}$$

The fibril at any layer in the twisted monofilament yarn in the strained condition will extend, and the fibril strain is written as

$$\begin{aligned} \varepsilon_t &= \frac{l_{t(\theta)}}{l_{0(\alpha)}} - 1 \\ &= \frac{h_t \sec\theta_t}{l_{0(\alpha)}} - 1 \end{aligned} \tag{2-6}$$

If the strain of the fibril at the neutral zone layer is written as

$$\varepsilon_{t(\alpha)} = \frac{l_{t(\alpha)}}{l_{0(\alpha)}} - 1 \tag{2-7}$$

then

$$l_{0(\alpha)} = \frac{l_{t(\alpha)}}{\varepsilon_{t(\alpha)}+1} = \frac{h_t \sec \alpha_t}{\varepsilon_{t(\alpha)}+1} \tag{2-8}$$

It had been calculated in the previous study[32] that the tensional force acting in the direction of the monofilament yarn axis was,

$$F_t = 2\pi \int_0^{R_t} E \left\{ \frac{\sec \theta_t}{\sec \alpha_t} (\varepsilon_{t(\alpha)}+1) - 1 \right\} r_t \cos^2 \theta_t dr_t \tag{2-9}$$

Again, assuming that the modulus of elasticity of the fibrils, E, are constant, then the solution of the above equation is (see Appendix),

$$F_t = \frac{E \varepsilon_{t(\alpha)} h_t^2 2(\sec \beta_t - 1)}{4\pi \left[1+\lambda_t^{-3} \left\{ \left(\frac{\sec \beta_0 - 1}{ln \sec \beta_0} \right)^2 - 1 \right\} \right]^{1/2}} \tag{2-10}$$

This becomes the correction to the Equation (22) in the previous study[32]. The nominal stress in the strained twisted monofilament yarn is calculated as

$$\sigma_t = \frac{F_t}{\pi R_0^2} \tag{2-11}$$

and the stress should be written as

$$\sigma_t = \frac{E \varepsilon_{t(\alpha)} h_t^2 2(\sec \beta_t - 1)}{4\pi^2 R_0^2 \left[1+\lambda_t^{-3} \left\{ \left(\frac{\sec \beta_0 - 1}{ln \sec \beta_0} \right)^2 - 1 \right\} \right]^{1/2}} \tag{2-12}$$

Since the monofilament yarn volume remains constant throughout twisting and tensioning, then considering Equations (2-3) and the constancy of monofilament yarn volume, then

$$\tan \beta_t = \frac{2\pi R_t}{h_t} = \frac{\tan \beta_0}{\lambda_t^{3/2}} = \frac{2\pi R_0}{h_0 \lambda_t^{3/2}} \tag{2-13}$$

and Equation (2-12) becomes

$$\sigma_t = \frac{E \varepsilon_{t(\alpha)} 2\lambda_t^2 \left\{ \left(\frac{\tan^2 \beta_0}{\lambda_t^3} + 1 \right)^{1/2} - 1 \right\}}{\tan^2 \beta_0 \left[1+\lambda_t^{-3} \left\{ \left(\frac{\sec \beta_0 - 1}{ln \sec \beta_0} \right)^2 - 1 \right\} \right]^{1/2}} \tag{2-14}$$

or it can be simply written as

$$\sigma_t = E\,\varepsilon_{t(\alpha)} K \tag{2–15}$$

where $E\,\varepsilon_{t(\alpha)}$ is a true stress. Since this value approximates to the nominal stress, Equation (2–15) is written as

$$\sigma_t = \sigma_i K \tag{2–16}$$

where σ_t represents the nominal stress in the twisted monofilament yarn, σ_i represents the nominal stress in the initial monofilament yarn, and

$$K = \frac{2\lambda_t^2 \left\{ \left(\frac{\tan^2 \beta_0}{\lambda_t^3} + 1 \right)^{1/2} - 1 \right\}}{\tan^2 \beta_0 \left[1 + \lambda_t^{-3} \left\{ \left(\frac{\sec \beta_0 - 1}{ln \sec \beta_0} \right)^2 - 1 \right\} \right]^{1/2}}$$

Now, the stress-strain curve of the twisted monofilament yarn can be determined from the initial yarn stress-strain curve for the given value of λ_t and the known surface helix angle β_0 by employing Equations (2–1) and (2–5) for calculating the extension ratio and Equation (2–16) to calculate the corresponding stress. The nominal stress has a unit quantity of g/mm^2, or g/cm^2. For the textile materials it is convenient to work in terms of the nominal specific stress measured in g/denier. In the denier system, the relation between nominal stress (g/cm^2) and nominal specific stress (g/den) is

$$1\ \frac{\text{g}}{\text{cm}^2} = \frac{1}{(9.10^5\,\rho)}\ \frac{\text{g}}{\text{denier}} \tag{2–17}$$

ρ is the monofilament yarn density. In term of nominal specific stress the Equation (2–16) becomes

$$\sigma_t = \sigma_i K C \tag{2–18}$$

where

$$C = \frac{1}{(9.10^5\,\rho)}$$

2.4 On the two-ply and three-ply cords

2.4.1 The doubly wound helix

The 'doubly wound helix' is the mathematical model postulated by Treloar[3] to describe the path of any filament in a cord construction. This mathematical model can be described briefly as follows. A simple helix may be regarded as generated by a rotating vector of length r advancing at constant rate $d\varphi/dz$ along the axis OZ (Fig. 2.3). The helix is completely defined by the magnitude of r and the angle α between the tangent to the helix and the z-direction. If n is the number of turns of the helix per unit length of axis then

$$\tan \alpha = 2\pi nr \tag{2-19}$$

The length of the helix, per unit length of axis, is

$$h = \sec \alpha = (1+4\pi^2 n^2 r^2)^{1/2} \tag{2-20}$$

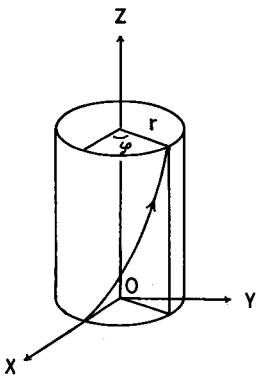

Fig. 2.3. Path of a simple helix.

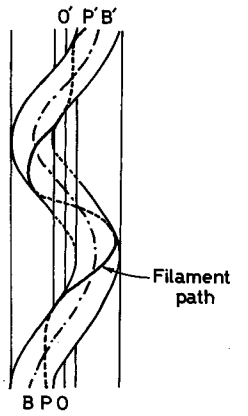

Fig. 2.4. Path of filament in the ply as a doubly wound helix.

The construction of a cord of 2, 3 or more single yarns or plies is symmetrically disposed about the cord axis. Since the plies are identical in form, only one of them need to be considered. The path of any filament in a multiply cord is a 'doubly wound helix' which is generated by the tip of a (secondary) vector of fixed length r rotating at a constant rate as its base moves along a simple helix (ply axis) at a constant rate; the ply axis being generated by the tip of another (primary) vector of fixed length a which also rotates at a constant rate as it moves along a straight line (cord axis) at a constant rate. The plane of rotation of the secondary vector is always at right angles to the ply axis. Such a ply is represented in Fig. 2.4, in which OO' represents the cord axis, BB' the ply axis, and PP' the individual filament. The ply axis is assumed to have the form of a simple helix of radius r and angle α. The relation between cord twist N and cord helix angle α is, from Equation (2–19),

$$\tan \alpha = 2\pi Na \tag{2-21}$$

It is necessary now to introduce some assumptions to provide a definition of the path of the filament. By analogy to the simple helix, which may be defined by means of a rotating vector as described in Fig. 2.3 it will assumed that the path of the filament in the ply may be generated by means of a rotating vector of length r advancing at constant rate along the helical ply axis. For convenience, we may measure the position of the vector r by the angle φ, referred to the principal plane of curvature of the point considered. Our fundamental assumption then becomes

$$\frac{d\varphi}{dl} = \text{constant} \tag{2-22}$$

where l is the distance measured along the ply axis.

Twist and torsion.

In textile literature, the quantity n (turns per unit length) is called the twist. Mathematically, it is frequently convenient to define the helix in term of the angular rate of rotation of the vector r. This quantity will be called the torsion τ of the helix. Hence

$$\tau = 2\pi n \tag{2-23}$$

Twist in ply.

Equation (2–22) is adequate for the specification of the state of twist in a single yarn. In the case of a ply in cord, however, the ply axis is no longer straight and the consideration of the state of twist in this case is more involved. The comparable problem in elasticity theory has been discussed by Love, A.E.H.[33]

The ply axis is itself a twisted (i.e., non-planar) curve, the principal plane of curvature at the point P, defined as the plane containing the tangents at the point P and the neighbouring point P′, rotates as P moves along the curve. The rate of rotation of the plane of curvature is called the tortuosity of the curve. In Love's nomenclature the symbol Σ is used for the reciprocal of the tortuosity. It is convenient to define the position of the filament in the ply by the angle φ, measured with respect to the principal plane of curvature of the ply axis at the point considered. The torsion with respect to the plane of curvature is then

$$\tau = \frac{d\varphi}{dl} \tag{2-24}$$

and the total torsion is

$$\tau_0 = \tau + \frac{1}{\Sigma} = \frac{d\varphi}{dl} + \frac{1}{\Sigma} \tag{2-25}$$

Equation (2–25) states that the total torsion is the sum of the torsion relative to the plane of curvature, and the rate rotation of the plane of curvature. In the cases when the ply axis is itself a helix having radius a and angle α, the tortuosity is given by

$$\frac{1}{\Sigma} = \frac{1}{a} \sin\alpha \cos\alpha \tag{2-26}$$

The Equation (2–25) is valid only in the case if there was no change in length of the ply axis during cording. In general, however, the length of the ply axis changes during cording. If the length of the ply axis before and after cording are l_i and l_0 respectively, then Equation (2–25) becomes

$$\tau_0 = \tau \frac{l_i}{l_0} + \frac{1}{a} \sin\alpha \cos\alpha \tag{2-27}$$

The ply axis length is given by Treloar as the solution of a quadratic equation, which is modified by Riding, $G^{8)}$ to the more general solution as

$$l = [-(2+gu) + 2(1+gu+u^2)^{1/2}]\frac{1}{u^2}\,. \tag{2-28}$$

where

$$g = \frac{2}{\frac{1}{2}b\tau}\left[\left(1+\frac{1}{4}b^2\tau^2\right)^{1/2} - 1\right] \tag{2-29}$$

and

$$u = \frac{\frac{1}{2}b}{a}\sin\alpha\cos\alpha \tag{2-30}$$

where b is the ply diameter.

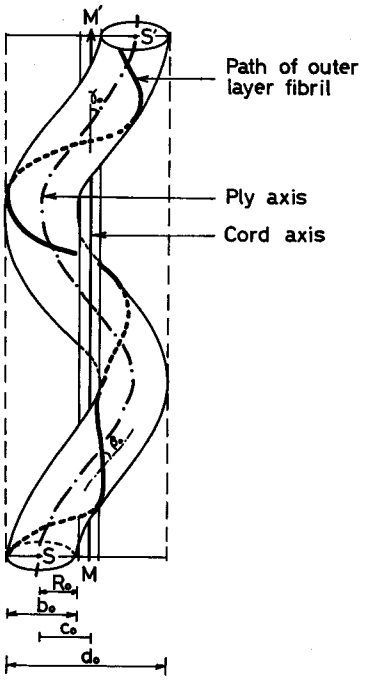

Fig. 2.5. Geometry of monofilament yarn as ply in the cord.

2.4.2 Geometry of strain and stress

On the two-ply and three-ply cord single-yarn strand

In the case of the twisted monofilament the problem was to calculate the strain in the fibril at the neutral zone layer as a function of the yarn axial extension. In the present case, the extension ratio of cord is calculated as a function of the ply axis extension ratio and the ply axis helix radius. The ply is itself a twisted monofilament and its extension ratio is determined from its relation with the initial yarn extension ratio and the helix angle of fibril at the surface of the twisted monofilament yarn. This magnitute of the ply surface helix angle is determine by calculating the torsion in the ply after cording process. If the total torsion in the ply is τ_0, then the helix angle at the surface of the ply is (See Fig. 2.5)

$$\beta_0 = \tan^{-1}\left(\frac{b_0}{2}\tau_0\right) \tag{2-31}$$

where the torsion in the ply is determined using Equation (2-27) which when referring to the principal symbols used becomes

$$\tau_0 = \frac{p}{p_0}\tau + \frac{1}{c_0}\sin\gamma_0\cos\gamma_0 \tag{2-32}$$

where p is the ply length before cording (=1.0), and τ is its torsion. The cord helix angle is represented as

$$\gamma_0 = \tan^{-1}(c_0\tau_{c0}) \tag{2-33}$$

and the ply length after cording is calculated as

$$p_0 = [-(2+gu) + 2(1+gu+u^2)^{1/2}]\frac{1}{u^2} \tag{2-34}$$

where

$$g = \frac{2}{\frac{1}{2}b_0\tau}\left[\left(1+\frac{1}{4}b_0^2\tau^2\right)^{1/2} - 1\right] \tag{2-35}$$

and

$$u = \frac{\frac{1}{2}b_0}{c_0}\sin\gamma_0\cos\gamma_0 \tag{2-36}$$

The helix angle of the fibril at the neutral zone layer of the ply is calculated using Equation (2-1), and the relation between the ply axis extension ratio, λ_t, and the initial monofilament yarn extension ratio written as λ_i is represented by Equation (2-5).

Cord extension ratio.

As in the case of single yarn, according to the assumption of the constancy of volume during tensioning, the ply radius in the strained state will be

$$\frac{1}{2}b_t = \frac{\frac{1}{2}b_0}{\lambda_t^{1/2}} \tag{2-37}$$

As the ply sections were circular, the ply radius and the cord helix radius are calculated as follows.

For two-ply cord,

$$c_0 = \frac{d_0}{4} = \frac{b_0}{2} \tag{2-38}$$

where d_0 is the diameter of cord.

For three-ply cord,

$$c_0 = \frac{1}{2}b_0\left(1+\frac{1}{3}\sec^2\gamma_0\right)^{1/2} \tag{2-39}$$

Yamamoto, K.[34] found that the Equation (2–39) is being regarded to be valid until about $\gamma_0=30°$.

If the shape of the ply axis is assumed to be unaffected by the strain, then the ply axis helix radius of the cord before and after strained relates as

$$c_t = \frac{c_0}{\lambda_t^{1/2}} \tag{2–40}$$

If τ_{co} and τ_{ct} represent the torsion of the cord before and after straining respectively, γ_0 and γ_t are its corresponding helix angles thus,

$$\tan \gamma_0 = c_0 \tau_{co} \tag{2–41}$$

and

$$\tan \gamma_t = c_t \tau_{ct} \tag{2–42}$$

If λ_c represents the extension ratio of the cord, then

$$\tau_{ct} = \frac{\tau_{co}}{\lambda_c} \tag{2–43}$$

From the Equations (2–40), (2–42) and (2–43) we obtain

$$\tan \gamma_t = \frac{\tau_{co}}{\lambda_c} \cdot \frac{c_0}{\lambda_t^{1/2}} \tag{2–44}$$

or we can write the Equation (2–44) as

$$\tan \gamma_t = \frac{\tan \gamma_0}{\lambda_c \lambda_t^{1/2}}$$

To obtain the relation between λ_t and λ_c we consider the cord axial length. We have then

$$\lambda_t = \frac{\text{strained ply axis length}}{\text{unstrained ply axis length}} = \frac{\lambda_c \sec \gamma_t}{\sec \gamma_0} \tag{2–45}$$

From the Equations (2–44) and (2–45) we can obtain

$$\lambda_t^2 \sec^2 \gamma_0 = \lambda_c^2(1+\lambda_c^{-2}\lambda_t^{-1} \tan^2 \gamma_0)$$

or

$$\lambda_c^2 = \lambda_t^2 \sec^2 \gamma_0 - \lambda_t^{-1} \tan^2 \gamma_0 \tag{2–46}$$

This equation enables λ_c to be obtained for the given values of λ_t and the calculated γ_0 from the know value of τ_{co}, while Equation (2–5) is for calculating the initial yarn extension ratio.

Stress in the cord.

In the application of the theoritical calculations representing the stress in

yarn, strand and cord, it is convenient to work in terms of the nominal specific stress rather than in true or absolute stress. In this study the calculation of stress will be done in term of the nominal specific stress with the unit of g/denier. The theory developed for calculating the stresses disregards the lateral pressure that may exist between plies.

If F_p is the force acting along the ply axis in the direction of the ply axis itself, then the force acting in the direction of the cord axis, F_{cp}, will be (Fig. 2.6)

$$F_{cp} = F_p \cos \gamma_t \qquad (2\text{–}47)$$

This force, F_{cp}, will become the contribution of the ply to the total force along the cord axis. For two-ply cord the total force acting in the cord in the direction of the cord axis becomes $2F_{cp}$ and for the three-ply cord, $3F_{cp}$.

The axial stress in the ply, σ_t, is calculated as

$$\sigma_t = \frac{C \cdot F_p}{\frac{1}{4}\pi b_0^2} \qquad (2\text{–}48)$$

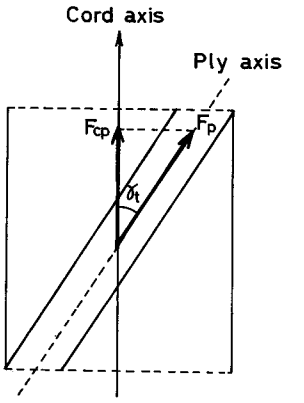

Fig. 2.6. Axial force acting in the cord of single-yarn strand.

where $C = \dfrac{1}{9.10^5 \rho}$, ρ is the material density.

The cord axial stress, σ_c, will be

$$\sigma_c = \frac{C \cdot F_{cp}}{\frac{1}{4}\pi b_0^2 \sec \gamma_0} = \frac{\sigma_t \cos \gamma_t}{\sec \gamma_0} \qquad (2\text{–}49)$$

Substitution of Equation (2–44) into (2–49) results

$$\sigma_c = \sigma_t \left(1 + \frac{\tan^2 \gamma_0}{\lambda_c^2 \lambda_t}\right)^{-1/2} \cos \gamma_0 \qquad (2\text{–}50)$$

The stress in the ply which is a twisted monofilament is obtained from the initial monofilament yarn stress using Equation (2–18). For the corresponding strain of cord, the stress in the cord can be calculated from the initial yarn stress using Equations (2–18) and (2–50).

On the two-ply and three-ply cord multiply-yarn strand

Since the strand as ply in the cord in which its axis forms a helix wound about the cord axis, and the monofilament yarn as ply in the strand in which its axis forms a helix wound about the strand axis are assumed to have a stress-strain curve as if it

were in the straight condition, then the extension ratio of the cord and the strand are calculated with the method that is analogous to the method for the calculation of cord extension ratio of the cord of single-yarn strand.

From the configuration of the cord, i.e. cord diameter d_0, the upper twist N_0, the lower twist (of the ply before cording) n_0, the following parameters can be calculated. (See Fig. 2.7)

The cord torsion is calculated as

$$\tau_{co} = 2\pi N_0 \tag{2-51}$$

The ply torsion before cording is

$$\tau = 2\pi n_0 \tag{2-52}$$

The cord helix radius is calculated as follows.

For two-ply cord

$$c_0 = \frac{d_0}{4} \tag{2-53}$$

For three-ply cord

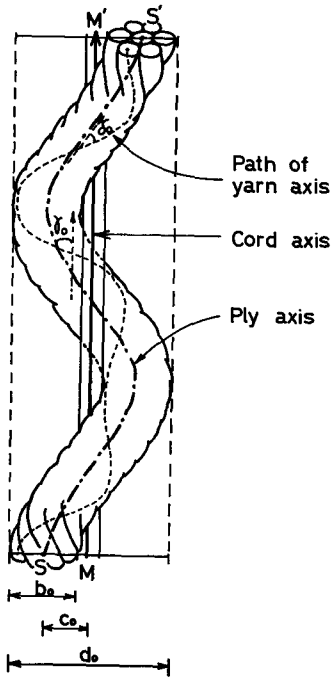

Fig. 2.7. Geometry of strand as ply in the cord.

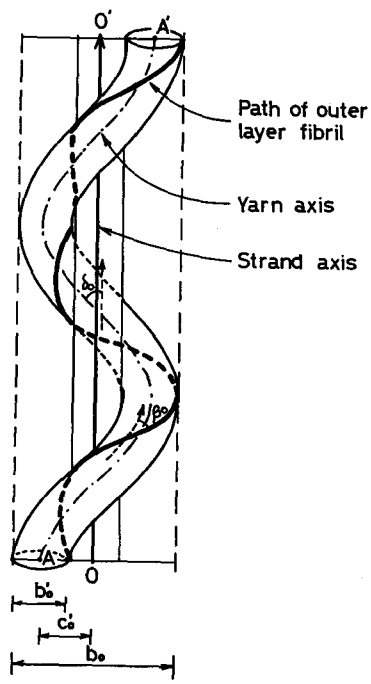

Fig. 2.8. Geometry of monofilament yarn as ply in the strand.

$$c_0 = \frac{b_0}{2}\left(1 + \frac{1}{3}\sec^2\gamma_0\right)^{1/2} \tag{2-53a}$$

The cord helix angle is calculated using Equation (2-33) as

$$\gamma_0 = \tan^{-1}(c_0\tau_{c0})$$

The ply diameter is calculated from the cord diameter as follows
For two-ply cord

$$b_0 = \frac{d_0}{2} \tag{2-54}$$

For three-ply cord

$$b_0 = d_0\left\{\left(1 + \frac{1}{3}\sec^2\alpha_0\right)^{1/2} + 1\right\}^{-1} \tag{2-54a}$$

The total torsion in the ply after the cording process is calculated using Equation (2-32) as

$$\tau_0 = \frac{p}{p_0}\tau + \frac{1}{c_0}\sin\gamma_0\cos\gamma_0$$

From the ply torsion value, τ_0, the angle of inclination of the monofilament yarn axis toward the strand axis can be calculated as (See Fig. 2.8),

$$\delta_0 = \tan^{-1}(c_0'\tau_0) \tag{2-55}$$

this calculation is refers to the monofilament yarn as ply in the outer layer of strand. From the configuration of the strand, the strand helix radius, c_0', can be determined as the distance of the yarn axis at the outer ply to the strand axis. If the radii of the monofilament yarns are assumed to be equal, then the strand helix radius is calculated as follows.
For 2-yarn strand

$$c_0' = R_0 = \frac{b_0}{4} \tag{2-56}$$

For 3-yarn strand

$$c_0' = R_0\left(1 + \frac{1}{3}\sec^2\delta_0\right)^{1/2} \tag{2-56a}$$

For 7-yarn strand

$$c_0' = \frac{b_0}{3} \tag{2-56b}$$

For 19-yarn strand

$$c_0' = \frac{2b_0}{5} \tag{2-56c}$$

Since the torsion of the monofilament yarn as ply in the strand before twisting operation on straind formation is zero, then the torsion of the monofilament yarn after strand formation is calculated as

$$\tau_0' = \frac{1}{c_0'} \sin \delta_0 \cos \delta_0 \tag{2-57}$$

and from this value, τ_0', we calculate the fibril helix angle at the surface of the monofilament yarn as

$$\beta_0 = \tan^{-1}(R_0 \tau_0') \tag{2-58}$$

The relation of the extension ratio of the initial monofilament yarn and the twisted yarn as ply in the strand is represented by Equation (2–5) written as

$$\lambda_i^2 = \frac{\lambda_t^2(1+\lambda_t^{-3} \tan^2 \alpha_0)}{\sec^2 \alpha_0}$$

and the fibril at the neutral zone layer helix angle is calculated using Equation (2–1), written as

$$\sec \alpha_0 = \frac{(\sec \beta_0 - 1)}{ln \sec \beta_0}$$

The extension ratio of the strand as ply in the cord λ_p, as well as the cord extension ratio λ_c, can be calculated using equations derived analogous to the derivation of Equation (2–46) and written as

$$\lambda_p^2 = \lambda_t^2 \sec^2 \delta_0 - \lambda_t^{-1} \tan^2 \delta_0 \tag{2-59}$$

and

$$\lambda_c^2 = \lambda_p^2 \sec^2 \gamma_0 - \lambda_p^{-1} \tan^2 \gamma_0 \tag{2-60}$$

Stress in the cord

The calculation of the stress of multiply-yarn strands is done after the calculation of stress in the strand. This is calculated from the relation with the corresponding stress acting in the monofilament yarn as the ply in the strand. Although the theoretical calculation of stress is developed without taking the effect of lateral pressure, however, the calculation of the stress acting in the strand will be executed refering to the monofilament yarn that lay in the outer ply. The stress in the monofilament yarn as ply in the strand is calculated using Equation (2–18), written as

$$\sigma_t = \sigma_i KC$$

The calculation of stress in the strand is done refering to the contribution of the force acting in the direction of the strand axis contributed by the monofilament yarn axial force in the outer ply (See Fig. 2.8). There will be no problem involved in the strand of 2-yarn and 3-yarn as all the individual yarns are identically disposed about the strand axis. In the case of 7-yarn strand, the strand consists of one thread of monofilament yarn as the core in the centre of the strand which is surrounded by 6 threads of monofilament yarn in the outer ply. In the cords of 19-yarn strands, each strand consists of one thread of monofilament yarn as the centre ply, 6 threads of monofilament yarn in the inner ply and 12 threads of monofilament yarn in the outer ply. Since the calculations on the extension ratio and the stress in the strand are refering to the outer ply, the geometry of stress in the monofilament yarn in the outer ply and its relation with the stress in the strand must be formulated. For the most practical purposes, the monofilament yarns may be considered to have circular sections of equal radii. The cross section area of the strand of 7-yarn construction then can be calculated as

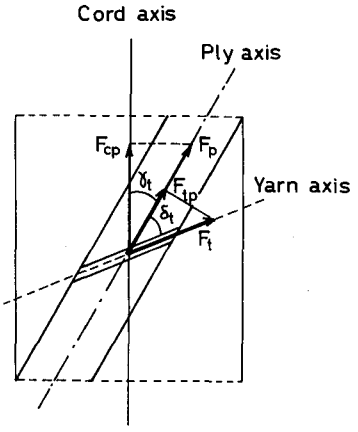

Fig. 2.9. Axial force acting in the cord of multiply-yarn strand.

$$A_0 = \pi R_0^2 + 6\pi R_0^2 \sec \delta_0 \qquad (2\text{–}61)$$

If F_p is the total force acting along the strand axis, then the axial stress in the strand is

$$\sigma_p = \frac{CF_p}{\pi R_0^2(1+6 \sec \delta_0)} \qquad (2\text{–}62)$$

If F_t is the force acting in each yarn in the outer ply, then the force that contributes to the total force acting in the strand from each yarn in the outer ply is (see Fig. 2.9)

$$F_{tp} = F_t \cos \delta_t \qquad (2\text{–}63)$$

With the proportionality of the cross section areas of the monofilament yarn and the strand perpendicular to the strand axis, this force, F_{tp} can be written as

$$F_{tp} = \frac{\pi R_0^2 \sec \delta_0}{\pi R_0^2(1+6 \sec \delta_0)} F_p = \frac{\sec \delta_0}{(1+6 \sec \delta_0)} F_p \qquad (2\text{–}64)$$

If the axial stress acting in each of monofilament yarn in the outer ply is σ_t, then

$$\sigma_t = \frac{CF_t}{\pi R_0^2} \qquad (2\text{–}65)$$

From the Equations (2-61) and (2-63) the axial stress acting in the strand can be calculated as follows

$$\sigma_p = \frac{CF_{tp}}{\pi R_0^2 \sec \delta_0}$$

or

$$\sigma_p = \frac{CF_t \cos \delta_t}{\pi R_0^2 \sec \delta_0} = \sigma_t \frac{\cos \delta_t}{\sec \delta_0} \tag{2-66}$$

In the case of 19-yarn strand, the strand axial stress is calculated as

$$\sigma_p = \frac{CF_p}{\pi R_0^2(1+6 \sec \delta_0' + 12 \sec \delta_0)} \tag{2-67}$$

where δ_0' is the helix angle of each monofilament yarn in the inner ply, and δ_0 is that in the outer ply. Regarding only the monofilament yarn in the outer ply, the force acting in the strand contributed by this yarn is

$$F_{tp} = F_t \cos \delta_t \tag{2-63}$$

where δ_t is the helix angle of each monofilament yarn axis in the outer ply with respect to the strand axis in the strained state.
This froce, F_{tp}, relates to the total force acting in strand, F_p, proportional with its cross section areas perpendicular to the strand axis, written as

$$F_{tp} = \frac{\pi R_0^2 \sec \delta_0}{\pi R_0^2(1+6 \sec \delta_0' + 12 \sec \delta_0)} F_p$$

$$= \frac{F_p \sec \delta_0}{(1+6 \sec \delta_0' + 12 \sec \delta_0)} \tag{2-68}$$

Substitution of Equations (2-65), (2-63) and (2-68) into (2-67) results

$$\sigma_p = \frac{CF_t \cos \delta t}{\pi R_0^2 \sec \delta_0} = \sigma_t \frac{\cos \delta_t}{\sec \delta_0} \tag{2-69}$$

In general, the Equations (2-66) and (2-69) represent the same expression for the relation of the stress in the outerply of the monofilament yarn and the stress in the strand for both 7-yarn strand and 19-yarn strand, written as

$$\sigma_p = \sigma_t \frac{\cos \delta_t}{\sec \delta_0}$$

The relation between δ_t and δ_0 can be calculated analogous with the derivation of the Equation (2-44), so that

$$\tan \delta_t = \frac{\tau_0'}{\lambda_p} \cdot \frac{c_0'}{\lambda_t^{1/2}} = \frac{\tan \delta_0}{\lambda_p \lambda_t^{1/2}} \tag{2-70}$$

or it can be written as

$$\sec \delta_t = \left(1 + \frac{\tan^2 \delta_0}{\lambda_p^2 \lambda_t}\right)^{1/2} \tag{2-71}$$

Substitution of Equation (2–71) into Equation (2–69) results

$$\sigma_p = \sigma_t \left(1 + \frac{\tan^2 \delta_0}{\lambda_p^2 \lambda_t}\right)^{-1/2} \cos \delta_0 \tag{2-72}$$

Now, the stress in the strand is obtained. The stress in the cord is calculated analogous to the calculation of stress in the cord for the cord of single-yarn strand represented by Equation (2–50) written as

$$\sigma_c = \sigma_p \left(1 + \frac{\tan^2 \gamma_0}{\lambda_c^2 \lambda_p}\right)^{-1/2} \cos \gamma_0 \tag{2-73}$$

Employing Equations (2–18), (2–72) and (2–73) we can calculate the cord axial stress if the values of twisted monofilament yarn extension ratio are given and the configuration of the cord is known.

3. Experimental techniques

3.1 On the two-ply and three-ply cord single-yarn strand

3.1.1 Materials and methods

Since in this study the samples are prepared by means of a twisting machine, the thinner the material is, the better it is for the machine to work with, but for the sake of getting more accurate measurements for the verification of the theory, experiments employing a large size of materials are desired. By this reason, Nylon–6 monofilament No. 16 with an average diameter of 0.659 mm was used as an adequate and proper type of yarn for the experiments.

In these experiments, the samples were prepared on a ring traveller type twisting machine. The procedure of the preparation of sample is described diagramatically in Fig. 3.1. The monofilament yarns are set in A (see also Fig. 3.2) so that it can roll freely when stretched. The formation of a single yarn strand is done by twisting only one thread of monofilament yarn. The yarn is stretched from A passing over the horizontal bars B and C, passing through rollers D (see also Fig. 3.3) to attain the desired tension by pressing the rollers to each other, hooked on the traveller E and attached to the bobbin G (see also Fig. 3.4). When the bobbin is rotated at a high speed by means of the motor H, the traveller E will travel along the ring F to give the twisting process to the yarn. The ring with the traveller is moving upward and downward during the twisting operation so that the twisted yarn is dispersed regularly along the bobbin G. The desired number of twists is obtained by ajusting the rotation speed of the motor. The cording process is done by twisting 2 for 2-ply cord and 3 for 3-ply cord of twisted monofilament yarns in an opposite direction to the twist direction of single yarn.

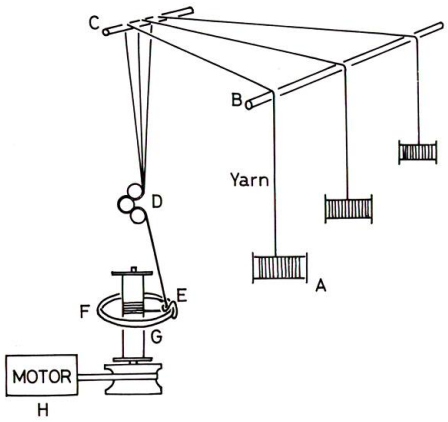

Fig. 3.1. Schematic diagram of ring traveller type twisting machine.
A; Bobbin, B; Horizontal bar; C; Horizontal bar, D; Rollers, E; Traveller, F; Ring, G; Rotating bobbin, H; Motor.

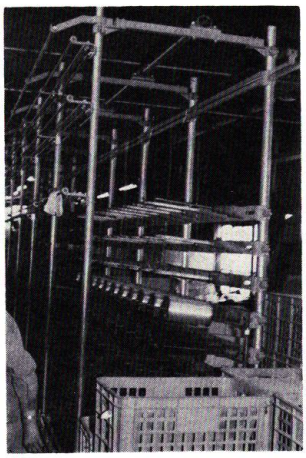

Fig. 3.2. Frame for setting the bobbin of yarn.

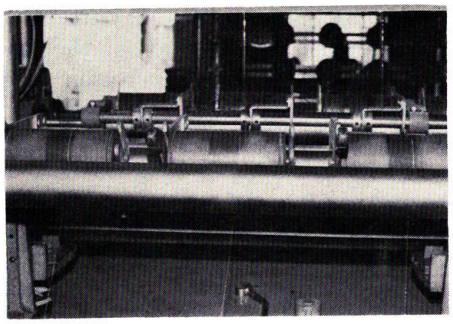

Fig. 3.3 Rollers to give tension to the yarn.

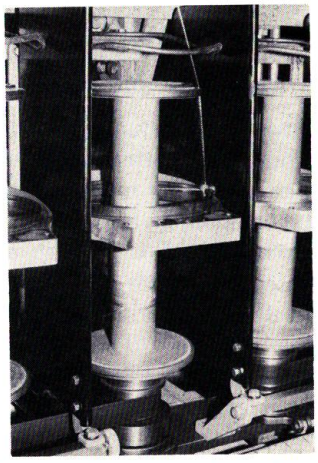

Fig. 3.4. Ring. traveller and rotating bobbin.

The number of twist were measured in turns per 6 inches of unit length. The helix angle at surface of cord is determined by using this following equation

$$\varphi_0 = \tan^{-1}\left(\frac{\pi d_0 N_0}{l}\right) \tag{3-1}$$

where φ_0 is the cord surface helix angle, N_0 is the cord twist number and l is the unit length (=6 inches), the cord diameter d_0, is measured using a profile projector.

At least 10 measurements were done to obtained the mean values. The configuration of the samples prepared in this machine are shown in Table 3.1.

The methods and apparatus for determining the stress-strain curve used in these experiments are the same with those used in the determination of the stress-strain curve of twisted monofilament yarn described in the previous study[32].

Table 3.1 Configurations of 2-play and 3-ply cord single-yarn strand

Sample number	Number of ply	Number of twist (turns/6 in)		diameter (mm)	helix angle (degree)
		upper*)	lower		
1	2	48.6 (50)	50	1.290	52.3
2	2	25.7 (25)	50	1.354	35.6
3	2	16.7 (17)	50	1.377	25.4
4	2	12.9 (13)	50	1.387	20.1
5	2	8.5 (8)	50	1.405	13.8
6	2	28.8 (30)	30	1.303	37.7
7	2	19.3 (20)	30	1.330	27.9
8	2	14.1 (15)	30	1.321	21.1
9	2	9.8 (10)	30	1.324	15.0
10	3	25.6 (25)	50	1.501	38.4
11	3	19.6 (20)	50	1.498	31.2
12	3	15.6 (15)	50	1.497	25.7
13	3	10.6 (10)	50	1.477	17.9
14	3	7.7 (7)	50	1.443	12.9
15	3	28.9 (30)	30	1.456	40.9
16	3	23.1 (23)	30	1.454	34.7
17	3	17.9 (18)	30	1.448	28.1
18	3	12.0 (12)	30	1.422	19.4
19	3	7.8 (8)	30	1.406	12.7

*) Values between brackets indicate the number of twist ajusted by the twisting machine while the other were obtained after recounting using an open up twister.

An example of a recorded load elongation curve is shown in the Fig. 3.5. The load elongation curve of every sample is drawn ten times, and about 8 to 15 points along each curve of a certain interval are taken to draw the stress-strain curve.

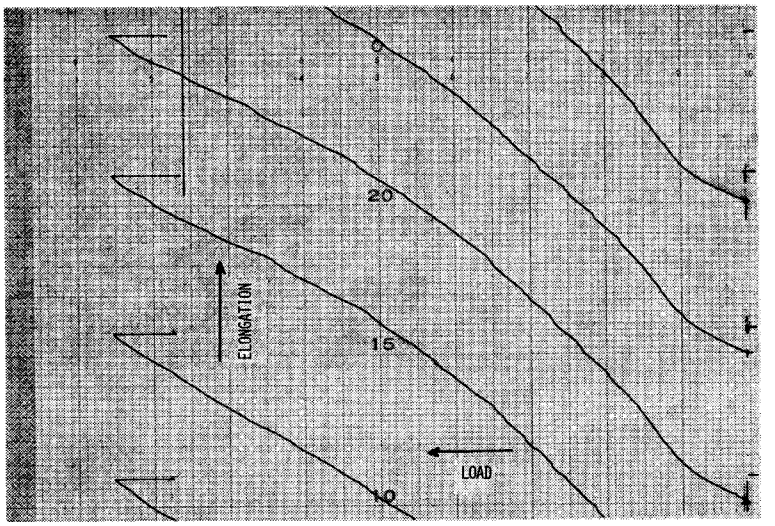

Fig. 3.5. An example of recorded data of load elongation curve.

The stress is calculated in terms of the nominal specific stress in g/denier. Ten values of each point are taken to obtain the mean value. For each sample an initial tension of about 1% of its breaking point is taken as the starting point of the load strain curve. At this point the stress and the strain values are regarded to be zero. The distance between chucks was 30.0 cm and the testing speed was 300 mm per minute. These experiments were carried out at room temperature varying from 20° to 25°C and at the relative humidity varying from 60% to 70%.

The denier count of the cords were obtained by measuring the weight of samples of each 1.00 m length by means of an electric balance with a capacity of 4000 g and and 0.01 g sensitivity. Ten measurements were done for each sample to obtain the mean values.

3.1.2 Results

Stress-strain curve determination

The stress-strain curve is presented with the strain value as a percentage and the stress in the nominal specific stress in g/denier. Fig. 3.6 represents the initial stress-strain curve of Nylon–6 monofilament No. 16.

From the cords stress-strain curves it can be seen that with the increasing cord surface helix angle the strain increase at the same tensile stress value, and with the increase of degrees of twisting in the cord construction it can be shown that the

strain increased and the tensile stress decreased. The comprehensive stress-strain curves of the cords are shown in the following figures. Fig. 3.7 and Fig. 3.8 represent the stress-strain curves of two-ply cord single-yarn strand at various cord surface helix angles with a different degree of twisting in the lower twist. Fig. 3.9 and Fig. 3.10 represent those of the cords of 3-ply construction.

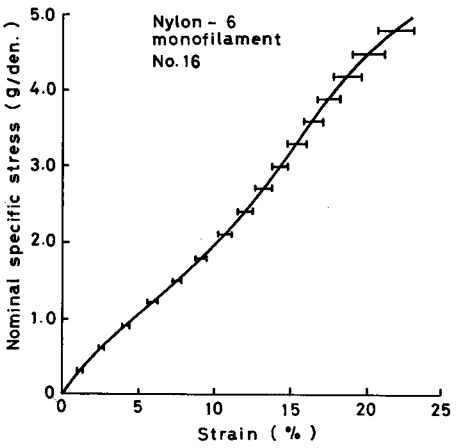

Fig. 3.6. Stress-strain curve of nylon-6 monofilament No. 16.
|—| ; minimum-maximum values range.

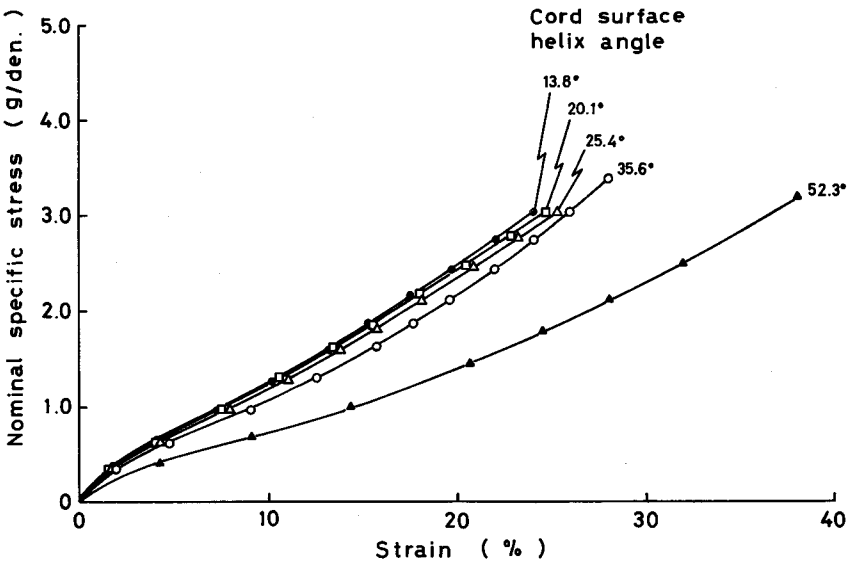

Fig. 3.7. Stress-strain curves of 2-ply cord single-yarn strand of 50 turns per 6 in. lower twist at various degrees of twisting.

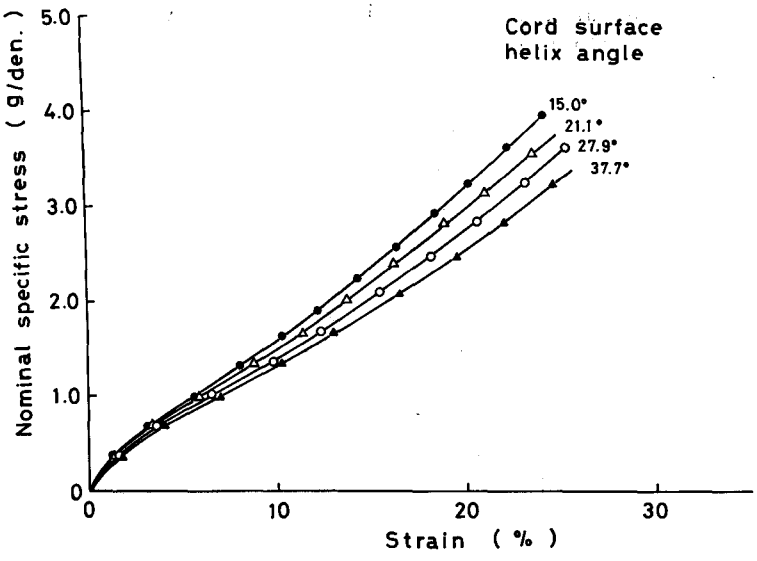

Fig. 3.8. Stress-strain curves of 2-ply cord single-yarn strand of 30 turns per 6 in. lower twist at various degrees of twisting.

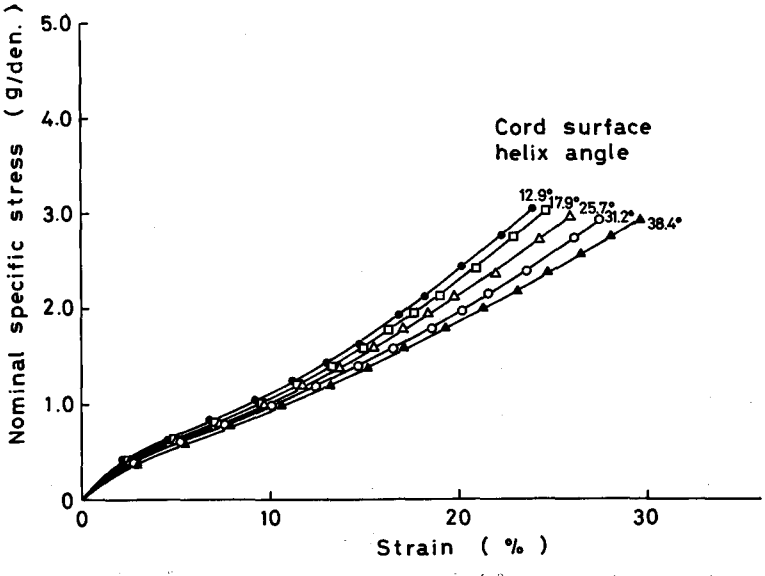

Fig. 3.9. Stress-strain curves of 3-ply cord single-yarn strand of 50 turns per 6 in. lower twist at various degrees of twisting.

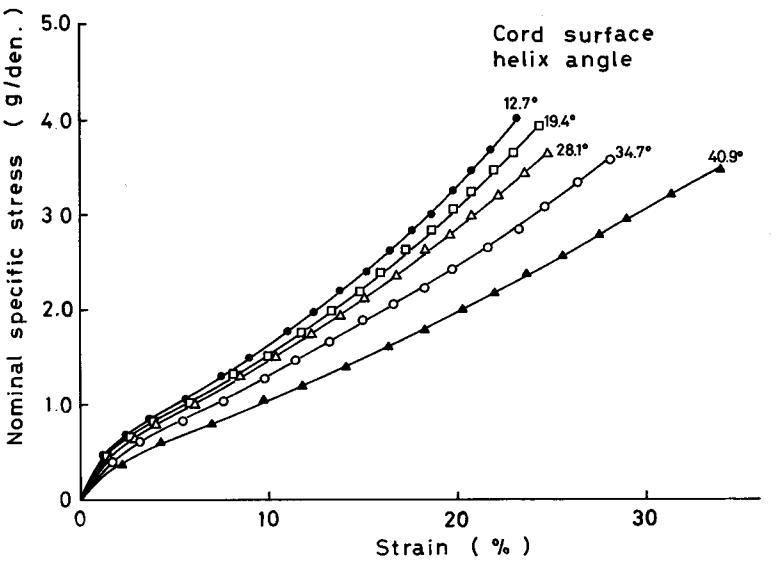

Fig. 3.10. Stress-strain curves of 3-ply cord single-yarn strand of 30 turns per 6 in. lower twist at various degrees of twisting.

3.2 On the two-ply and three-ply cord multiply-yarn strand

3.2.1 Materials and methods

Material used in these experiments were of Nylon–6 monofilament No. 8. with an average diameter of 0.497 mm. This material was thought to be the proper and adequate material for making samples since the samples are made over a wide range of cords constructed of 4 threads of monofilament yarns to 57 threads of monofilament yarns.

Before the samples used for the determination of the stress-strain curves were constructed, experiments on the strand retraction ratio were done. The procedure of the experiments are described diagramatically in Fig. 3.11. The monofilament yarns were stretched from the head of the hand driller A (see also Fig. 3.12), passing through the holes in the plate B (Fig. 3.13), and passing over the pulleys C (see Fig.

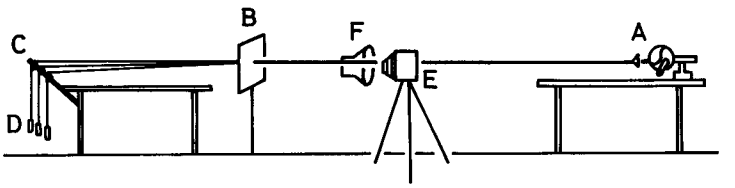

Fig. 3.11. Schematic diagram of apparatus for twisting the strand and cord.
A; Simple hand driller, B; Plate with holes, C; Pulleys, D; Weights, E; Camera, F; Light.

3.14) so that the yarns were stretched horizontally at the desired tension by means of the weight D. The twisted monofilament yarns were photographed using a camera at every certain interval of number of turns in order to measure the diameter of the twisted yarns. These were done subsequently by means of a profile projector. This work was done for 2, 3, 7, and 19-ply of single yarns. The twisting operations were done until the snarling process almost happened.

The preparation of strands and cords were done using the same apparatus and methods as described in Fig. 3.11 diagramatically. The distance between the hand driller and the plate was 12.0 m, and the distance between plate and the pulleys was about 2.0 m. The strands of equal number of single yarns as its plies were prepared in three different surface helix angle of about 20°, 30°, and 40°. For each kind of strand 2-ply and 3-ply constructions of cords were made. These were carried out using the same apparatus and methods of strand formation, by applying the strands instead of monofilament yarns. The direction of twist in the cord was the opposite to the twist in the strand. The configuration of samples (strands and cords) made

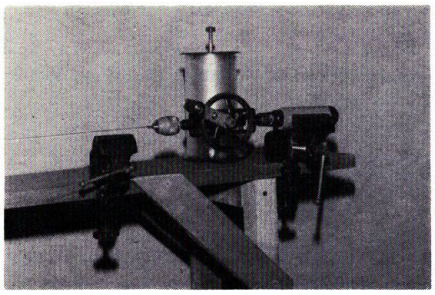

Fig. 3.12. Hand driller.

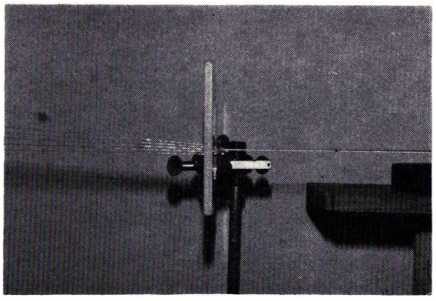

Fig. 3.13. Plate with holes.

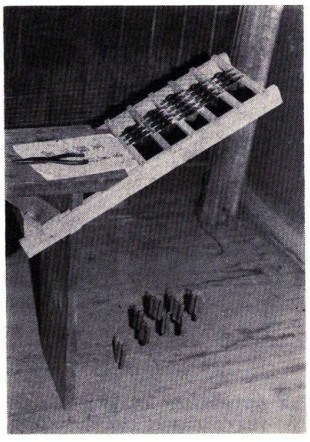

Fig. 3.14. Pulleys and weights.

Table 3.2 Configurations of 2-play and 3-ply cord multiply-yarn strand

No.	Sample number	Ply number configuration	Number of twist (turns/m)		diameter (mm)	surface helix angle (degree)
			upper	lower		
1	1	7	—	103.5	1.441	25.1
2	4	7	—	165.5	1.543	38.7
3	7	7	—	80.8	1.485	20.6
4	10	3	—	234.4	1.046	38.4
5	13	3	—	176.6	1.031	29.7
6	16	3	—	117.8	1.016	20.4
7	19	19	—	94.6	2.467	38.4
8	22	19	—	71.0	2.601	30.1
9	25	19	—	47.3	2.603	21.2
10	28	2	—	276.1	0.955	39.6
11	31	2	—	197.2	0.953	30.5
12	34	2	—	118.9	0.497	19.3
13	6	3/21	76.6	165.5	3.063	36.4
14	3	3/21	57.0	103.5	3.052	29.9
15	8	3/21	54.7	80.8	3.026	27.4
16	5	2/14	78.8	165.5	2.874	35.4
17	2	2/14	65.5	103.5	2.791	29.9
18	9	2/14	53.0	80.8	2.807	25.1
19	20	3/57	40.6	94.6	5.365	34.4
20	23	3/57	31.5	71.0	5.654	29.3
21	26	3/57	26.3	47.3	5.593	24.8
22	21	2/38	48.5	94.6	5.306	38.9
23	24	2/38	42.0	71.0	5.092	33.9
24	27	2/38	31.0	47.3	4.885	30.7
25	11	3/9	91.3	243.4	2.174	31.9
26	14	3/9	82.0	176.6	2.183	29.3
27	17	3/9	73.5	117.8	2.131	26.2
28	12	2/6	34.5	243.4	1.981	34.5
29	15	2/6	89.0	176.6	1.994	29.1
30	18	2/6	73.0	117.8	1.962	24.2
31	29	3/6	118.0	276.1	1.864	34.6
32	32	3/6	98.5	197.2	1.906	30.5
33	35	3/6	76.6	118.9	1.877	24.2
34	30	2/4	138.0	276.1	1.672	35.9
35	33	2/4	110.0	197.2	1.656	29.7
36	36	2/4	70.0	118.9	1.677	20.2

by this procedure are represented in Table 3.2. The surface helix angle of the cord and the diameter of the cord were determined by using the same procedure as described in Section 3.1.1.

The procedure and methods for determining the stress-strain curve of strands and cords were the same as those used in the determination of stress-strain curves of cords of single-yarn strand, described in Section 3.1.1.

In Chapter 2. section 2.4.2 the theory was developed considering the equality of radii for the individual monofilament yarns circular section in their position in the construction of strands and cords. To make observation on the actual situation,

cross-sectional shapes of these cords were examined by embedding them in coagulate so that a section could be cut without distorsion in the cross-section form, and these sections could be observed using a microscope. The coagulate used in these experiments was a polyester resin mixed with a hardner liquid. The proportion of the mixing ratio used in these experiments was 0.5 ml hardner for 20.0 ml of polyester. The procedure adopted was as follows. The specimen was passed through a plastic tube of 30 mm in diameter. This plastic tube had a hole in the centre of its base and a hole in the centre of its stopped in the upper end through which the specimen passed. The specimen was held so that its position was parallel to the axis of the tube. The hole in the base of the tube was covered with a cement agent to prevent any leak that may be happened. The prepared specimens were fixed in the strength testing machine so that any desired tension could be given. The embedding mixture then was poured into the tube and the upper end of the tube was close by a stopper. The tube containing the embedded specimen was left in a still condition for over 4 hours in room temperature in order for the mixture to set. After the mixture coagulated well, the embedded specimen could be removed from the plastic tube. The sectional view of cords were obtained by cross cutting the embedded specimen using an ordinary pad-saw and polishing it on a graind stone. These sections were observed under a binocular microcope and photographs were taken.

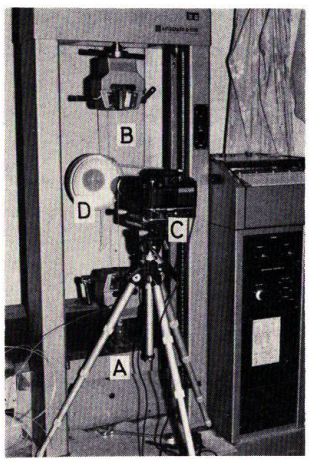

Fig. 3.15. Apparatus for the determination of the change of cord diameter by tension. A; Strength testing machine, B; Test piece, C; Camera, D; Light.

The measurements of the diameters of the cords and change in the diameter throughout tensioning made by the above procedure and method were not sufficient in order to make an interpretation, as they was limited to only a few of the available samples. Another method for determining the cord diameter change throughout tensioning was carried out. This was done by photographing the cord during tensioning (see Fig. 3.15). The measurement of the diameter of cord was done by observing the photograph under a profile projector.

3.2.2 Results

Stress-strain curve determination

From the stress-strain curves represented by the following figures below, it can be seen for the strand and cords that the values of the strains increase with an increasing twist in the strand or cords of the same tensile stress. In general the strain of the strand or cord increases and the stress decreases following an

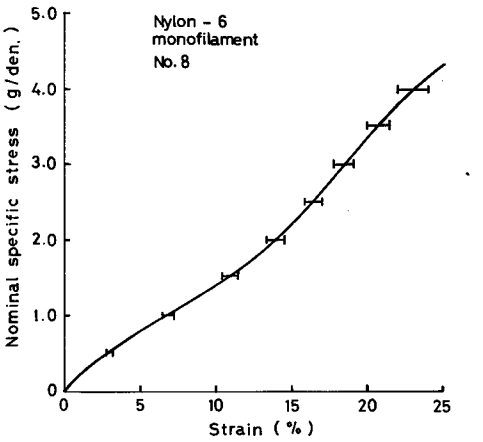

Fig. 3.16. Stress-strain curve of Nylon-6 monofilament No. 8.
|—| minimum-maximum values range.

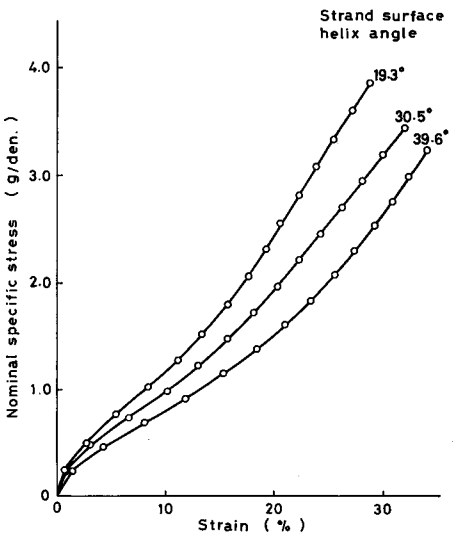

Fig. 3.17. Stress-strain curves of 2-yarn strand at various degrees of twisting.

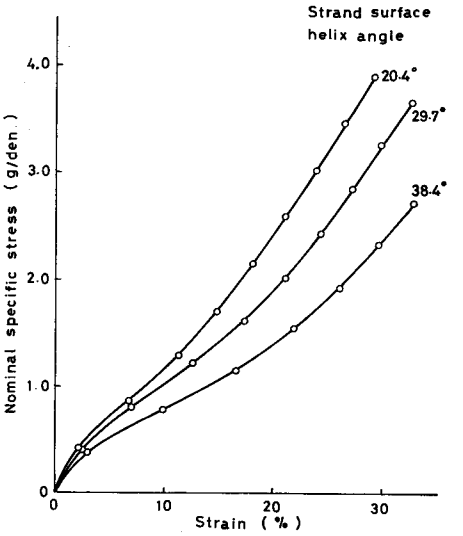

Fig. 3.18. Stress-strain curves of 3-yarn strand at various degrees of twisting.

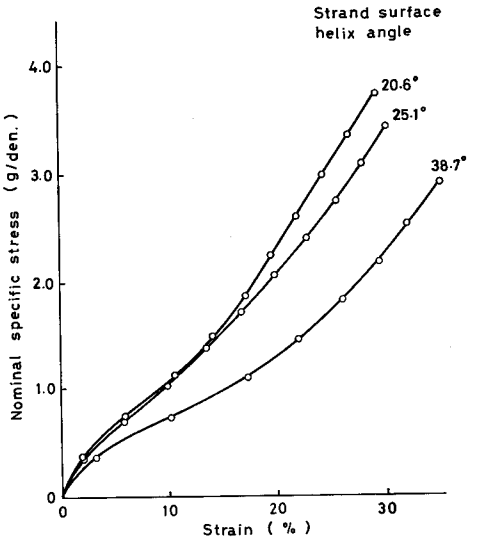

Fig. 3.19. Stress-strain curves of 7-yarn strand at various degrees of twisting.

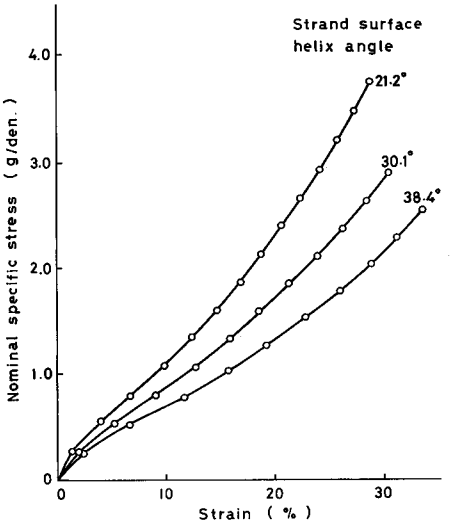

Fig. 3.20. Stress-strain curves of 19-yarn strand at various degrees of twisting.

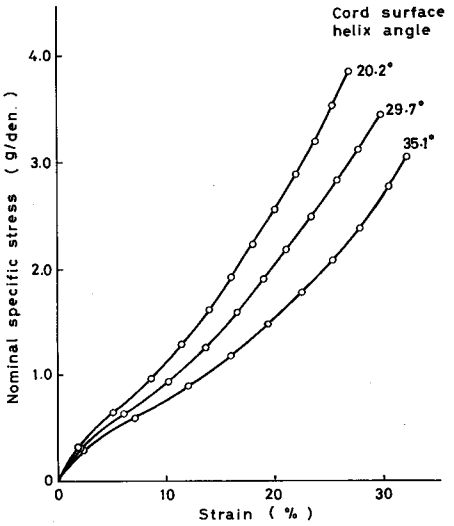

Fig. 3.21. Stress-strain curves of 2-ply cord 2-yarn strand at various degrees of twisting.

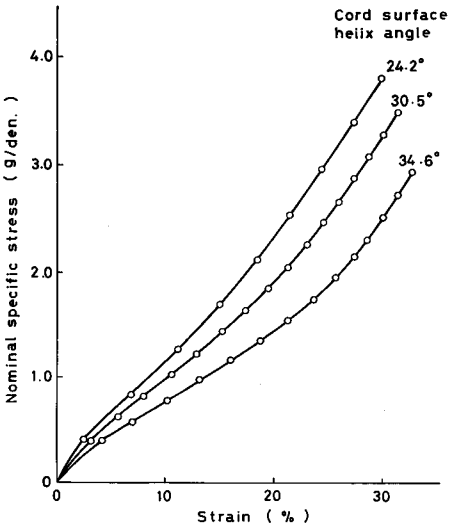

Fig. 3.22. Stress-strain curves of 3-ply cord 2-yarn strand at various degrees of twisting.

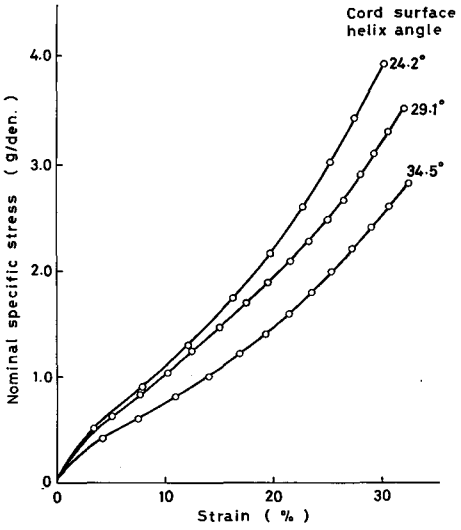

Fig. 3.23. Stress-strain curves of 2-ply cord 3-yarn strand at various degrees of twisting.

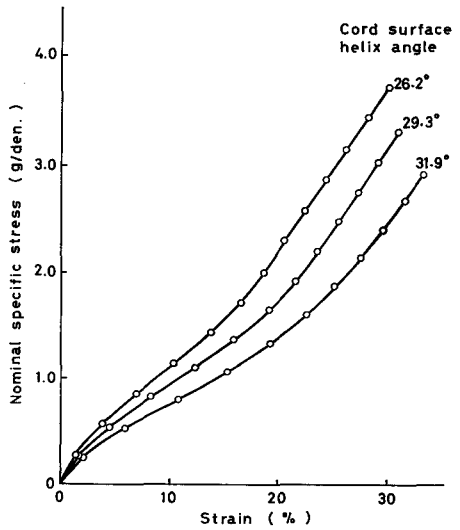

Fig. 3.24. Stress-strain curves of 3-ply cord 3-yarn strand at various degrees of twisting.

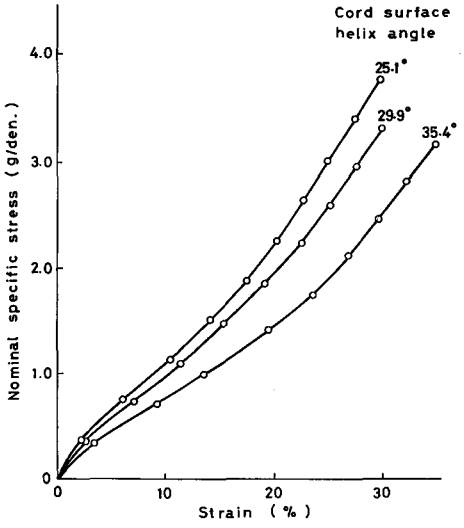

Fig. 3.25. Stress-strain curves of 2-ply cord 7-yarn strand at various degrees of twisting.

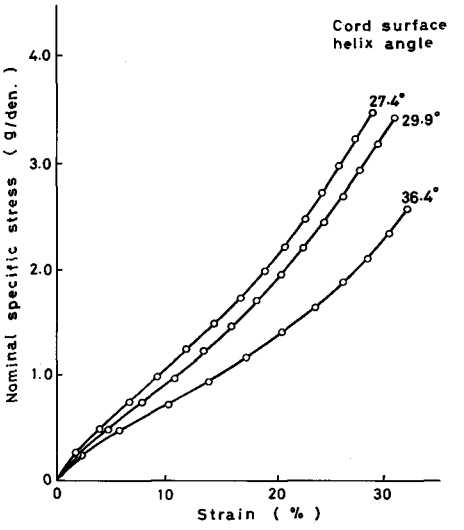

Fig. 3.26. Stress-strain curves of 3-play cord 7-yarn strand at various degrees of twisting.

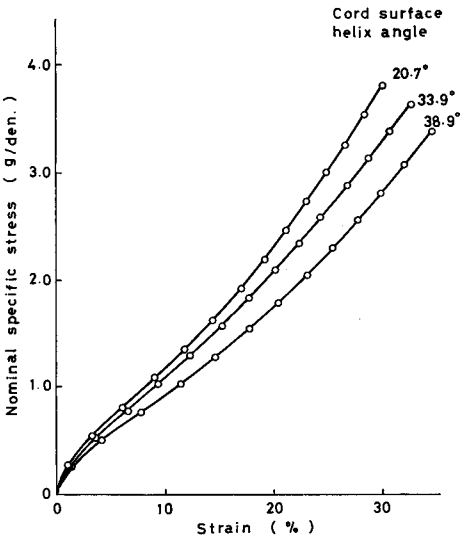

Fig. 3.27. Stress-strain curves of 2-ply cord 19-yarn strand at various degrees of twisting.

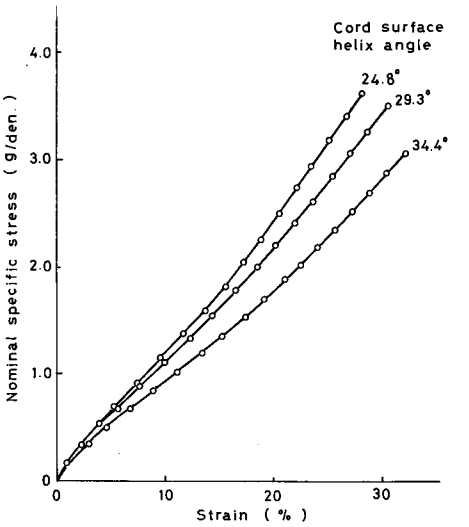

Fig. 3.28. Stress-strain curves of 3-ply cord 19-yarn strand at various degrees of twisting.

increase of the degrees of twisting. Figure 3.16 represents the initial stress-strain curve of Nylon–6 monofilament No. 8. Fig. 3.17 up to Fig. 3.20 represent the stress-strain curves of the strand in various constructions, each with various strand surface helix angles. Fig. 3.21 up to Fig. 3.28 represent cord stress-strain curves of various constructions in various degrees of cord surface helix angles.

Observation on the cord cross section

The results of the observation on the cross sections of cords show the ellipse form of the individual yarn sections in the strand and cord, and it seem that the radii may be regarded as being equal. The section of strands as plies in the cord may be regarded as having circullar shapes particularly for strands constructed from 7 and 19 threads of yarn, but 2-yarn strands and 3-yarn strands show some irregularity. Throughout tensioning the individual yarns move closer to each other, the air spaces decrease or disappear and the individual yarn section shapes become irregular. These phenomena can be seen in the following figures below (Fig. 3.29 to Fig. 3.39). Measurement on diameters of cords, strands and individual yarns directly to the figures below show that during tensioning the cord diameters decrease until about 80% to 90% of the initial condition. The individual yarn diameter change could not hardly be seen. These phenomena are described in Fig. 3.40 and Table 3.3.

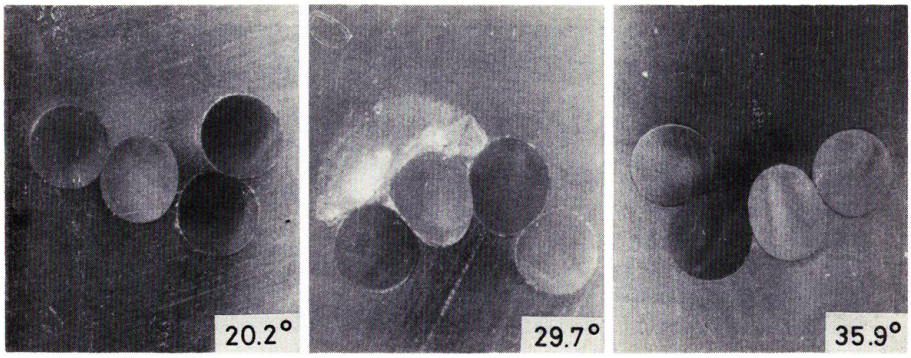

Fig. 3.29. Cross sections of 2-ply cord 2-yarn strand at various surface helix angles.

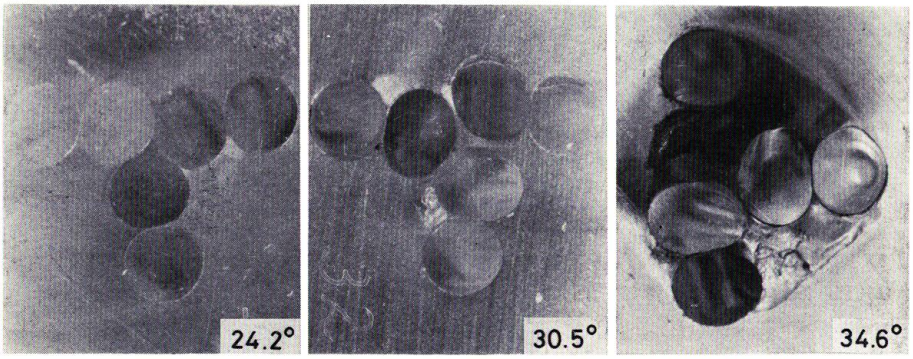

Fig. 3.30. Corss sections of 3-play cord 2-yarn strand at various surface helix angles.

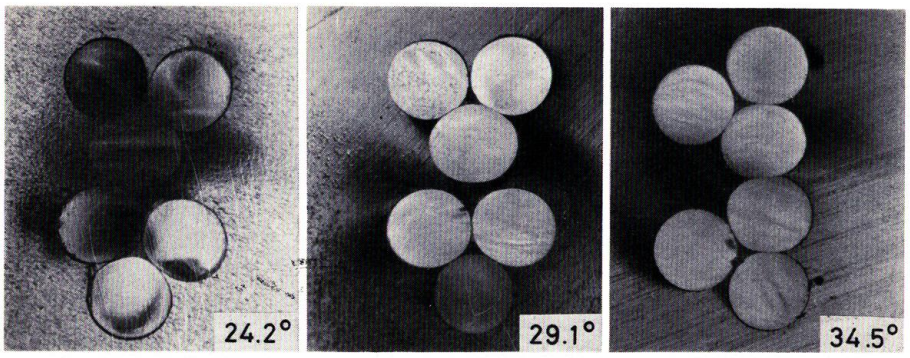

Fig. 3.31. Cross sections of 2-ply cord 3-yarn strand at various surface helix angles.

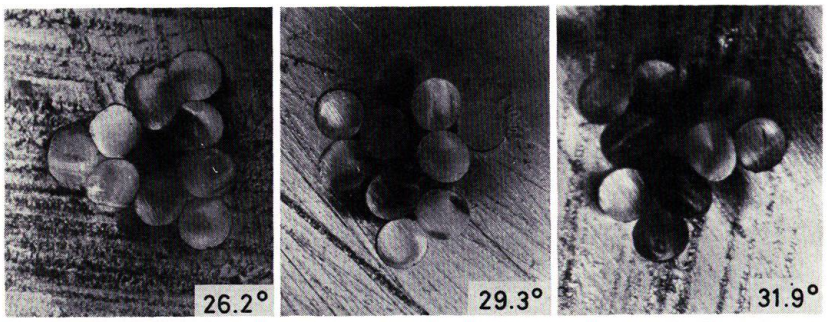

Fig. 3.32. Cross sections of 3-play cord 3-yarn strand at various surface helix angles.

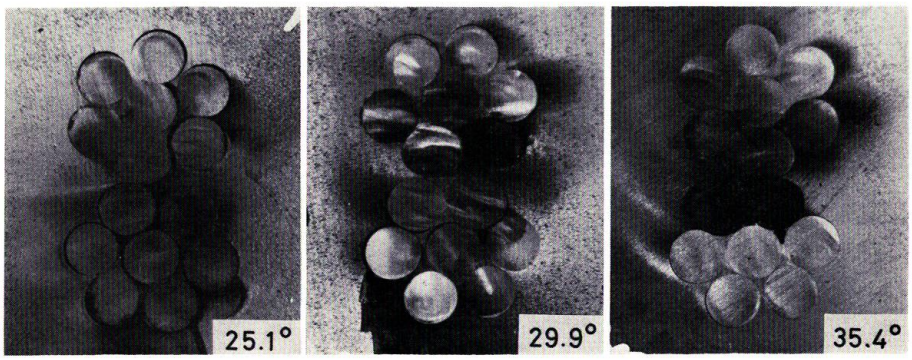

Fig. 3.33. Cross sections of 2-ply cord 7-yarn strand at various surface helix angles.

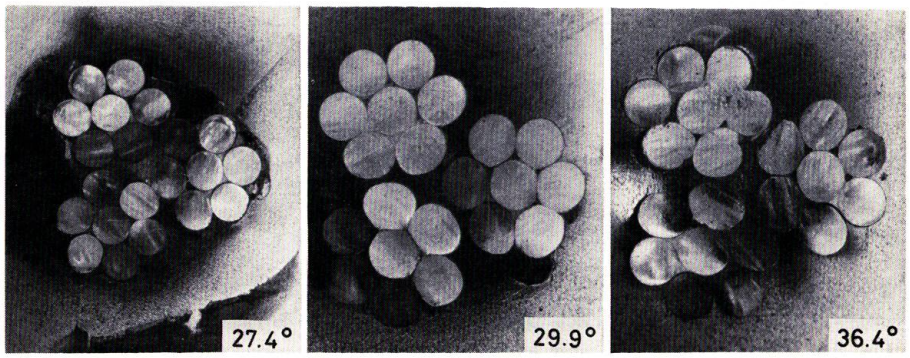

Fig. 3.34. Cross sections of 3-ply cord 7-yarn strand at various surface helix angles.

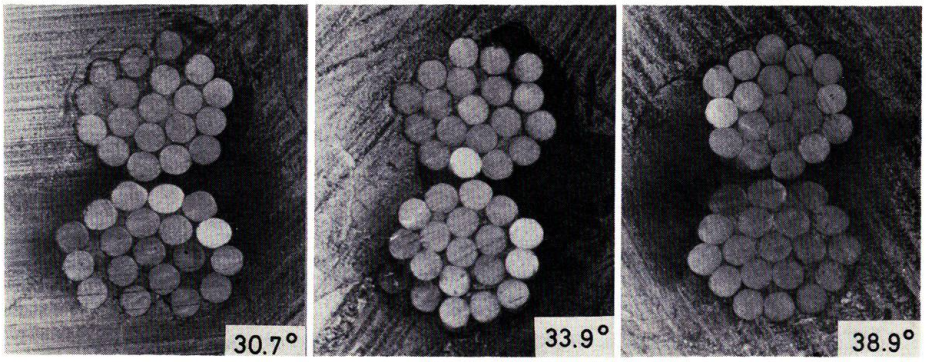

Fig. 3.35. Cross sections of 2-ply cord 19-yarn strand at various surface helix angles.

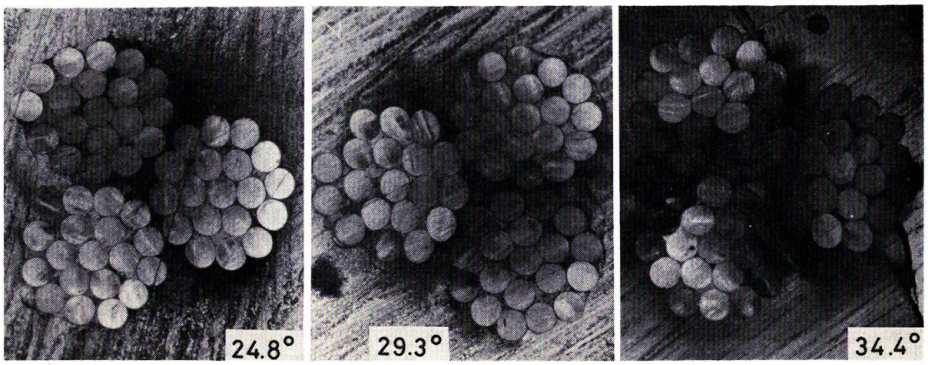

Fig. 3.36. Cross sections of 3-ply cord 19-yarn strand at various surface helix angles.

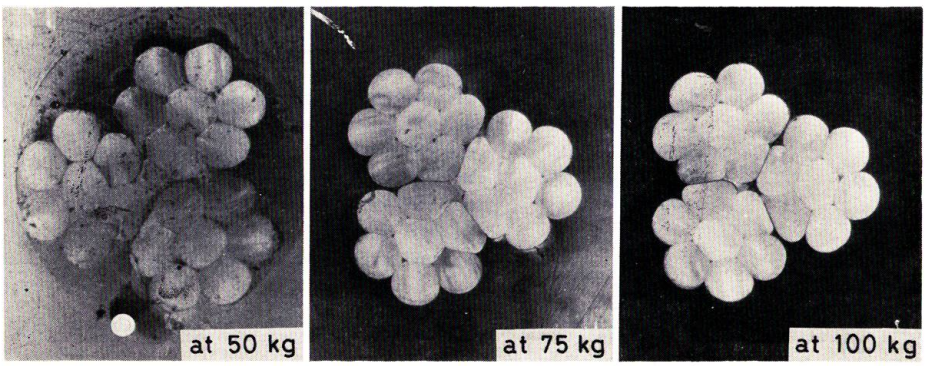

Fig. 3.37. Cross sections of 3-ply cord 7-yarn strand at various tensions.

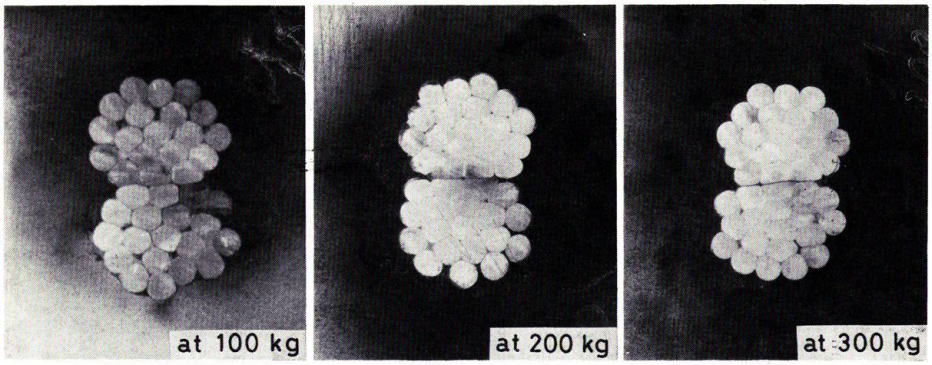

Fig. 3.38. Cross sections of 2-ply cord 19-yarn strand at various tensions.

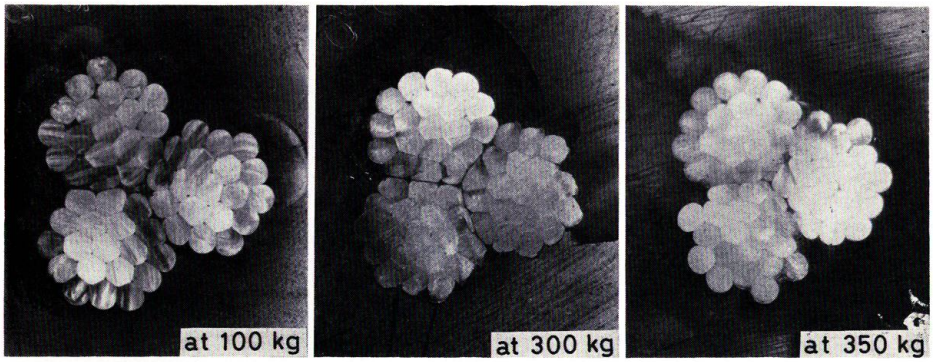

Fig. 3.39. Cross sections of 3-ply cord 19-yarn strand at various tensions.

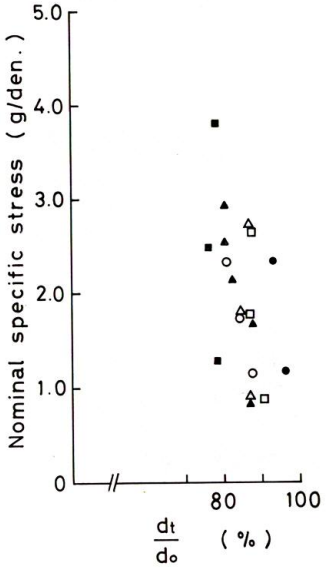

Fig. 3.40. Diameter change by tensions of cords of various configurations.
●; 3/21 with 36.4° surface helix angle,
○; 3/21 with 29.9° surface helix angle,
■; 2/38 with 38.8° surface helix angle,
△; 3/57 with 34.4° surface helix angle,
□; 3/57 with 29.3° surface helix angle,
▲; 3/57 with 24.8° surface helix angle.

Table 3.3 Cross sections of cords by tension

No.	Sample number	Cord configuration	tension (kg)	diameter		
				cord (mm)	ply (mm)	yarn (mm)
1	20	3/57	0	5.2	2.6	0.5
2	〃	〃	100	4.6	2.2-2.4	0.5
3	〃	〃	200	4.6	2.3-2.6	0.5
4	〃	〃	250	4.3	2.5	0.5
5	〃	〃	300	4.2	2.0-2.2	0.5
6	〃	〃	350	4.2	2.0-2.5	0.4-0.5
7	23	〃	0	5.2	2.4	0.5
8	〃	〃	100	4.8	2.3	0.5
9	〃	〃	200	4.6	2.2	0.5
10	〃	〃	300	4.6	2.2-2.8	0.5
11	26	〃	0	5.4	2.5-2.6	0.5
12	〃	〃	100	4.6	2.0 2.5	0.4-0.5
13	〃	〃	200	4.5	2.2-2.5	0.4-0.5
14	〃	〃	300	4.6	2.2-2.5	0.4-0.5
15	21	2/38	0	4.6	2.2-2.8	0.5
16	〃	〃	100	3.7	1.8-2.4	0.4-0.5
17	〃	〃	200	3.6	1.8-2.3	0.5
18	〃	〃	300	3.6	1.6-2.2	0.4
19	3	3/21	0	3.2	1.5	0.5
20	〃	〃	50	2.8	1.4	0.5
21	〃	〃	75	2.7	1.3-1.5	0.5
22	〃	〃	100	2.6	1.3-1.5	0.5
23	6	3/21	0	3.0	1.4-1.5	0.5
24	〃	〃	50	2.9	1.5	0.5
25	〃	〃	75	2.6	1.3-1.4	0.4-0.5
26	〃	〃	100	2.8	1.2-1.4	0.4-0.5

Diameter change by tension

Observation of the cord diameter change by tensional force are represented by the following figures (Fig. 3.41 to Fig. 3.45) describing the relation of tension and its change in diameter of various constructions of cord in the various degrees of cord surface helix angles. It can be seen that in general the diameter decreases with the increasing tensile stress. There are slight decreases by the increasing degrees of twist in the cord for the same tensile stress of the same cord construction.

Strand retraction ratio

The results of the determination of the strand retraction ratio is represented in Fig. 3.46. In this figure it can be seen that the shrinkage in the strand formation is increased with increasing the degree of twisting. For the same value of the degree of twisting the shrinkage of strand constructed by more considerable threads of monofilament yarns is larger than the strand constructed by less threads of monofilament yarns.

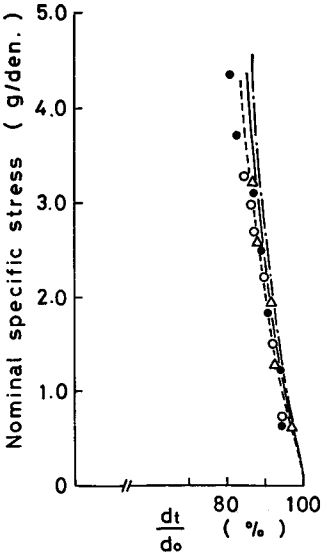

Fig. 3.41. Calculated and experimental values of diameter change by tensions of 2-ply cord 2-yarn strand at various surface helix angles.
△; experimental, -·-·-; calculated, for 20.2° surface helix angle,
●; experimental, ——; calculated, for 29.7° surface helix angle,
○; experimental, ----; calculated, for 35.9° surface helix angle.

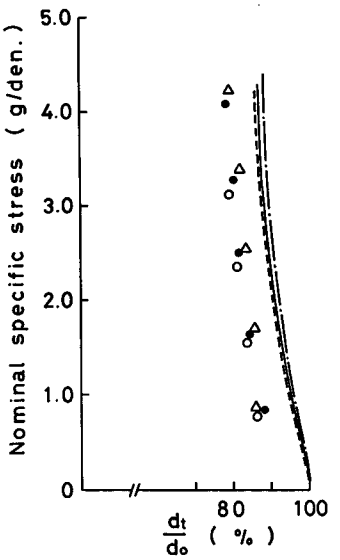

Fig. 3.42. Calculated and experimental values of diameter change by tensions of 3-ply cord 2-yarn strand at various surface helix angles,
experimental, -·-·-; calculated, for 24.2° surface helix angle,
●; experimental, ——; calculated, for 30.5° surface helix angle,
○; experimental, ----; calculated, for 34.6° surface helix angle.

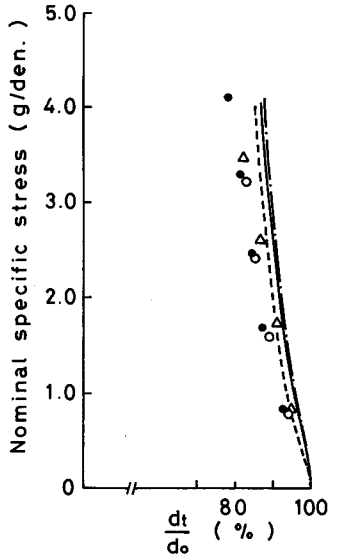

Fig. 3.43. Calculated and experimental values of diameter change by tensions 2-ply cord 3-yarn strand at various surface helix angles.
△; experimental -·-·-; calculated, for 24.2° surface helix angle,
●; experimental, ——; calculated, for 29.1° surface helix angle,
○; experimental, ----; calculated, for 34.5° surface helix angle.

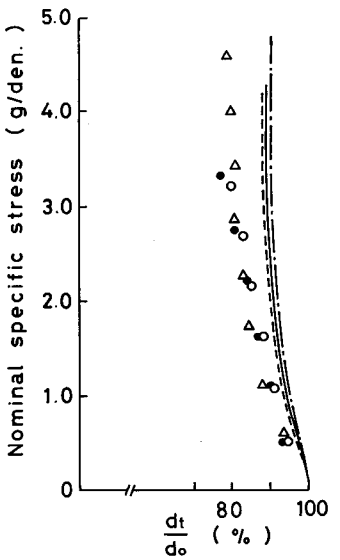

Fig. 3.44. Calculated and experimental values of diameter change by tensions of 3-ply cord 3-yearn strand at various surface helix angles,
△; experimental, -·-·-; calculated, for 26.2° surface helix angle,
●; experimental, ——; calculated, for 29.3° surface helix angle,
○; experimental, ----; calculated, for 31.9° surface helix angle.

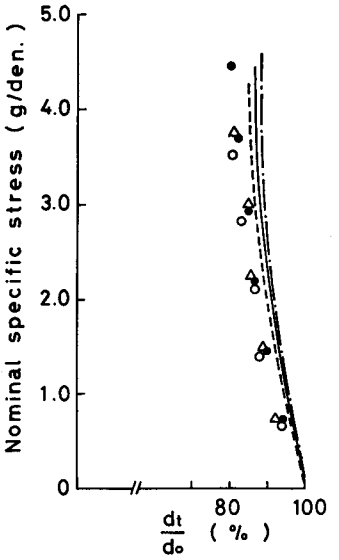

Fig. 3.45. Calculated and experimental values of diameter change by tensions of 2-ply cord 7-yearn strand at various surface helix angles,
△; experimental, -·-·-; calculated, for 25.1° surface helix angle,
●; experimental, ——; calculated, for 29.9° surface helix angle,
○; experimental, ----; calculated, for 35.4° surface helix angle.

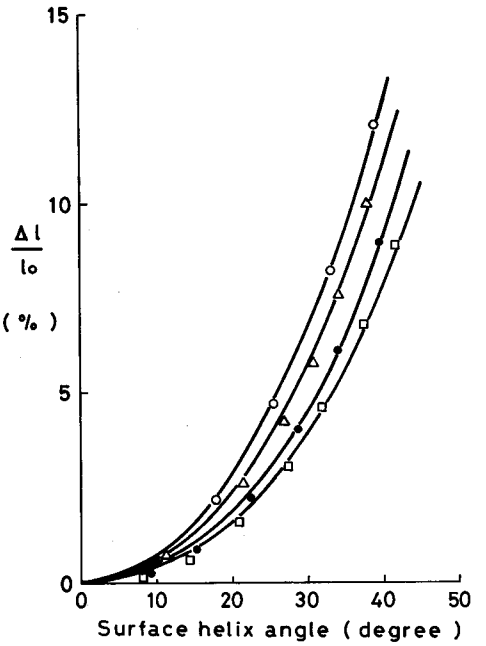

Fig. 3.46. Calculated and experimental values of strand retraction ratio.
□; 2-yarn strand, ●; 3-yarn strand, △; 7-yarn strand, ○; 19-yarn strand, solid-line: calculated values.

4. Comparison of theoretical calculations with experimental results

4.1 Strand retraction ratio

In Chapter 3 experiments were made to observe the change in length (shrinkage) of strand after and before the twisting operation done to form the strand from parallel monofilament yarns have been carried out. Theoretical calculation of strand retraction ratio is done based on the equality of individual monofilament yarn radii which make up the strand and the fact the shrinkage in this cases is proportioned to the ratio of the sum of the monofilament yarns cross section areas before and after formation into the strand.

If l_0 is the initial length of the individual monofilament yarns before strand formation and the length of the strand resulting from the twisting operation of the parallel initial yarns is l_s, then the mass of the strand before and after twisting operation is

$$l_0 A_0 \rho = l_s A_s \rho \tag{4-1}$$

where A_0 is the total yarn cross section area which form the strand before twisting operation, A_s is that after strand formation, and ρ is the material density.
The shrinkage, then, can be calculated as

$$\frac{\Delta l}{l_0} = \frac{l_0 - l_s}{l_0} = 1 - \frac{l_s}{l_0} = 1 - \frac{A_0}{A_s} \tag{4-2}$$

This equation represents the strand retraction ratio calculated from the yarn cross section area. The total yarn cross section in the strand is calculated as follows. For two-yarn strand

$$A_0 = 2\pi R_0^2 \tag{4-3}$$

and

$$A_s = 2\pi R_0^2 \sec \delta_0 \tag{4-4}$$

where R_0 is the monofilament yarn radius, δ_0 is the helix angle of the yarn axis with respect to the strand axis. This is calculated as

$$\delta_0 = \tan^{-1}(2\pi R_0 n) \tag{4-5}$$

where n is the twist of the strand.
Substitution of Equation (4-4) into (4-2) results in

$$\frac{\Delta l}{l_0} = 1 - \cos \delta_0 \tag{4-6}$$

For three-yarn strand

The ratio of A_0 and A_s is calculated as

$$\frac{A_0}{A_s} = \frac{3\pi R_0^2}{3\pi R_0^2 \sec \delta_0} = \cos \delta_0 \tag{4-7}$$

where the helix angle, δ_0, of yarn axis with respect to the strand axis is calculated as follows. If δ_s is the surface helix angle of the strand, c is the yarn axis helix radius as ply in the strand and n is the twist in the strand, then

$$\tan \delta_s = 2\pi n(c+R_0) \tag{4-8}$$

and

$$\tan \delta_0 = 2\pi nc \tag{4-9}$$

The ply helix radius is calculated as (analogous to Eq. 2-39)

$$c = R_0\left(1+\frac{1}{3}\sec^2 \delta_0\right)^{1/2} \tag{4-10}$$

and then, the relation between δ_0 and δ_s is calculated as

$$\tan \delta_0 = \frac{\tan \delta_s\left(1+\frac{1}{3}\sec^2 \delta_0\right)^{1/2}}{1+\left(1+\frac{1}{3}\sec^2 \delta_0\right)^{1/2}} \tag{4-11}$$

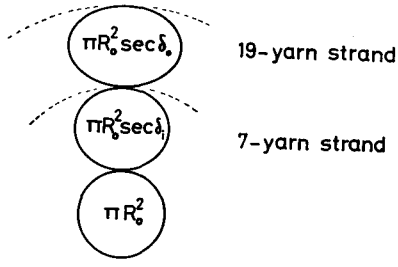

Fig. 4.1. Cross section area in individual monofilament yarn in the strand.

For 7-yarn strand. (See Fig. 4.1)

The ratio of A_0 and A_s is calculated as

$$\frac{A_0}{A_s} = \frac{7\pi R_0^2}{\pi R_0^2(1+6\sec \delta_0)} = \frac{7}{1+6\sec \delta_0} \tag{4-12}$$

where the helix angle δ_0 is calculated as follows. The 7-yarn strand has a construction of one thread of yarn in the centre and 6 threads of yarns in the outer ply. If δ_s is the strand surface helix angle, since the yarns are equal in radii, then δ_0 can be calculated as

$$\tan \delta_0 = \frac{2}{3}\tan \delta_s \tag{4-13}$$

For 19-yarn strand (See Fig. 4.1).

In the case of 19-yarn strand the formation of yarns in the strand will consist of one thread of yarn in the centre, 6 threads in the inner ply and 12 threads of yarn in the outer ply. If the helix angle of yarn axis in the inner ply is δ_i the helix angle of yarn axis in the outer ply is δ_0 and δ_s is the strand surface helix angle, then the ratio of A_0 and A_s is calculated as

$$\frac{A_0}{A_s} = \frac{19\pi R_0^2}{\pi R_0^2(1+6 \sec \delta_i + 12 \sec \delta_0)}$$

or

$$\frac{A_0}{A_s} = \frac{19}{1+6 \sec \delta_i + 12 \sec \delta_0} \tag{4-14}$$

where δ_i and δ_0 are calculated as

$$\tan \delta_i = \frac{2}{5} \tan \delta_s \tag{4-15}$$

and

$$\tan \delta_0 = \frac{4}{5} \tan \delta_s \tag{4-16}$$

The comparison between the experimental results and the calculation values of the strand retraction ratio show a good agreement except in the small values of strand surface helix angle. Strands with more considerable yarns give better agreement than strands of less individual yarns. This phenomena is represented in Fig. 3.46.

4.2 Diameter change by tension

To make a comparison of theory with an experiment on the diameter change of cord by tension, the theoretical calculation is done as follows. If c_0 is the cord helix radius before straining and c_t is that after straining then analogous to the equation (2-40), it can be written

$$c_t = \frac{c_0}{\lambda_p^{1/2}} \tag{4-17}$$

The ratio of the cord diameter before and after tension is applied is proportional to the ratio of the cord helix angle before and after straining. In the case of two-ply cord these ratios remain in the same proportion before and after straining so that

$$\frac{d_t}{d_0} = \frac{c_t}{c_0} = \frac{1}{\lambda_p^{1/2}} \tag{4-18}$$

where d_0 is the cord diameter before straining and d_t is that in the strained state.

For three-ply cord the ratio of d_t and d_0 is calculated as follows.
Since it is analogous to Equation (2–39), the cord helix radius is written as

$$c_0 = \frac{b_0}{2}\left(1 + \frac{1}{3}\sec^2\gamma_0\right)^{1/2}$$

where b_0 is the ply diameter, and that

$$d_0 = 2\left(c_0 + \frac{b_0}{2}\right) \tag{4-19}$$

then

$$d_0 = 2c_0\left(1 + \left(1 + \frac{1}{3}\sec^2\gamma_0\right)^{-1/2}\right) \tag{4-20}$$

The ratio of d_t and d_0 can then be written as

$$\frac{d_t}{d_0} = \frac{c_t\left(1 + \left(1 + \frac{1}{3}\sec^2\gamma_t\right)^{-1/2}\right)}{c_0\left(1 + \left(1 + \frac{1}{3}\sec^2\gamma_0\right)^{-1/2}\right)} \tag{4-21}$$

The relation between γ_t and γ_0 is calculated by using Equation (2–44), which can be written as

$$\sec\gamma_t = \left(\frac{\tan^2\gamma_0}{\lambda_c^2\lambda_p} + 1\right)^{1/2} \tag{4-22}$$

Substitution of Equation (4–17) into (4–21) results in

$$\frac{d_t}{d_0} = \frac{\left(1 + \left(1 + \frac{1}{3}\sec^2\gamma_t\right)^{-1/2}\right)}{\lambda_p^{1/2}\left(1 + \left(1 + \frac{1}{3}\sec^2\gamma_0\right)^{-1/2}\right)} \tag{4-23}$$

The relation of the stress σ_c and its corresponding diameter ratio d_t/d_0, calculated by Equation (4–23), is compared with the experimental results. These comparisons shows that the experimental values of diameter ratio before and after straining are smaller than the theoretical calculations particularly for the high tensile stress except for cords constructed from 2-yarn strand. This may be due to the disregarding of the change of the ply shapes during tensioning as the results of the transverse force. These phenomena are shown in Fig. 3.41 up to Fig. 3.45.

4.3 Stress-strain curve

On the cords of single-yarn strand.

The calculation procedure to obtain the stress-strain curve of cord in this

case is first to calculate the value of helix angle of fibril at the neutral zone layer of the tiwsted monofilament yarn as the ply in the cord from the configuration of the cord. Then in order to derive the stress-strain curve of the twisted yarn, derivation is done analogous with that of the twisted monofilament yarn described before, and after that it remain left to derive the stress-strain curve of the cord. This can be described as follows.

(1) Determination of ply surface helix angle β_0 using Equations (2–31), (2–32), (2–33), (2–34), (2–35), (2–36) and (2–38) or (2–39).

(2) Determination of fibril helix angle at the neutral zone layer α_0 using Equation (2–1)

Then, the derivation of stress-strain curve of cord from the initial yarn stress-strain curve is done as follows (See Fig. 4.2)

(3)—(4) Calculation of λ_i from the given value of λ_t and the obtained α_0, using Equation (2–5)

(4)—(5) Determination of stress σ_i from the initial yarn curve.

(5)—(6) Determination of σ_t from σ_i using Equation (2–18)

(3)—(7) Calculation of λ_c using Equation (2–46) from the given λ_t and γ_0 obtained using Equation (2–41).

(6)—(8) Calculation of σ_c from σ_t using Equation (2–50)

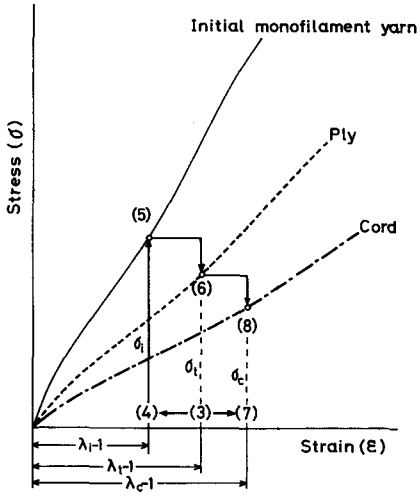

Fig. 4.2. Procedure of calculation of stress-strain curve of cord of single-yarn strand from the initial monofilament yarn stress-strain curve.

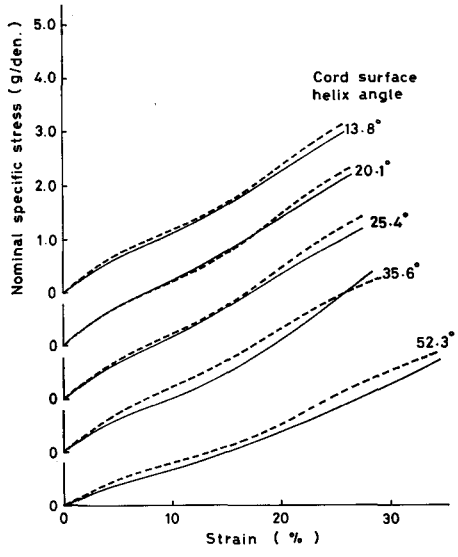

Fig. 4.3. Calculated and experimental stress-strain curves of 2-ply cord single yarn strand of 50 turns per 6 in. lower twist at various degrees of twisting.
solid line; experimental, broken line; calculted.

Table 4.1 Numerical example to determine the stress-strain curve of 2-ply cord single yarn strand of 1.29 mm diameter, 48.6 turns per 6 in. upper twist (Z), 50 turns per 6 in lower twist (S) and $\alpha_0=8.5°$.

λ_t	λ_i	λ_c	σ_i (gr/den)	σ_c (gr/den)
1.00	1.00	1.00	0.00	0.00
1.02	1.02	1.03	0.05	0.34
1.04	1.04	1.06	0.89	0.60
1.06	1.06	1.09	1.22	0.82
1.08	1.08	1.13	1.54	1.03
1.10	1.10	1.16	1.90	1.26
1.12	1.12	1.19	2.36	1.55
1.14	1.14	1.21	2.88	1.87
1.16	1.16	1.24	3.43	2.20
1.18	1.17	1.27	3.70	2.33
1.20	1.19	1.30	4.22	2.66
1.22	1.21	1.33	4.63	2.88
1.24	1.23	1.36	4.96	3.05
1.26	1.25	1.38	5.12	3.12

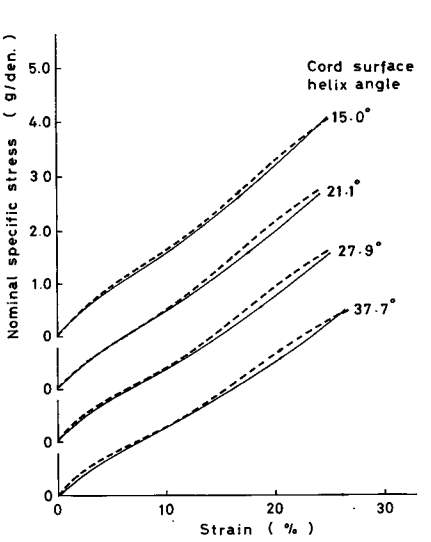

Fig. 4.4. Calculated and experimental stress-strain curves of 2-ply cord single-yarn strand of 30 turns per 6 in. lower tiwst at various degrees of twisting.
solid line; experimental, broken line; calculated.

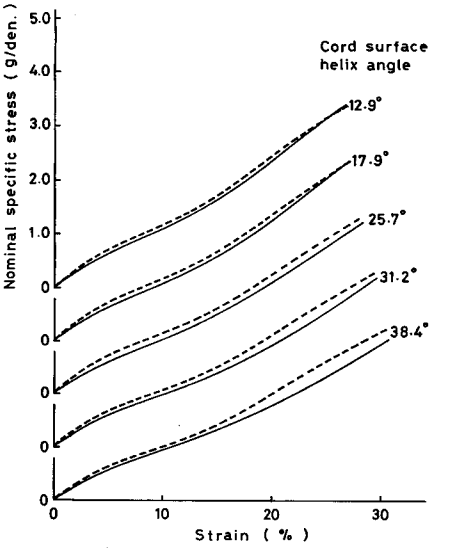

Fig. 4.5. Calculated and experimental stress-strain curves of 3-ply cord single yarn strand of 50 turns per 6 in. lower twist at various degrees of twisting.
solid line; experimental, broken line; calculated.

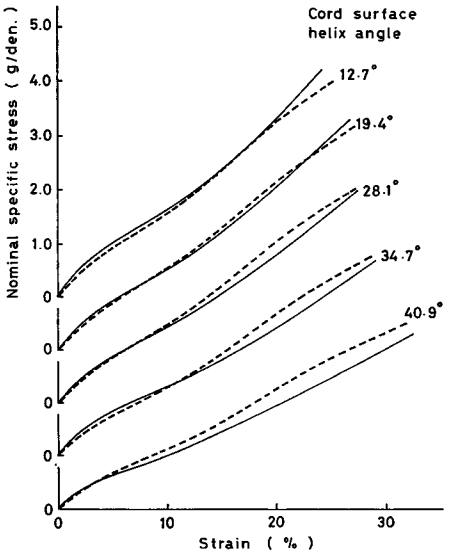

Fig. 4.6. Calculated and experimental stress-strain curves of 3-ply cord single yarn strand of 30 turns per 6 in. lower twist at various degrees of twisting.
solid line; experimental, broken line; calculated.

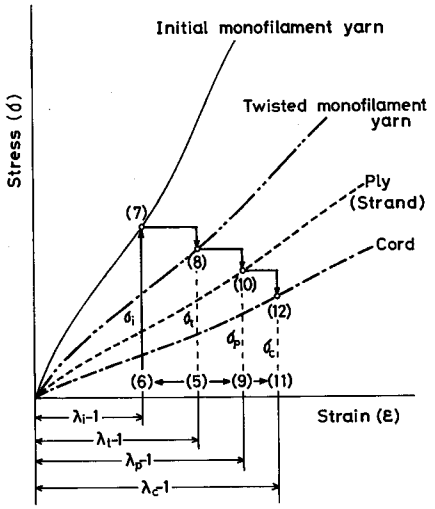

Fig. 4.7. Procedure of calculation of the stress-strain curve of cord of multiply-yarn strand from the initial monofilament yarn stress-strain curve.

The stress-strain curve of twisted monofilament yarn as ply in the cord is not drawn in the figure. Numerical example for the two-ply cord single yarn strand stress-strain relationship is given in Table 4.1. The results of stress-strain curve calculation in general agrees well with the experimental curve although a slight deviation still exists. It can be seen that the calculated curve deviates from the experimental curve to a larger value of stress at the same condition of strain. Representative figures are given below (Fig. 4.3–Fig. 4.6).

On the cords of multiply-yarn strand.

The procedure of calculation of cord stress-strain curve is first to calculate the strand stress-strain curve with the analogy procedure adopted for the cord of single-yarn strand stress-strain curve calculation. Then this is to be continued by the derivation of the cord stress-strain curve from the obtained strand stress-strain curve. Procedure of this calculation from the known configuration of the cord is described as follows.

(1) Calculation of cord helix angle γ_0 by employing Equations (2–33), (2–53) or (2–53a), (2–54) or (2–54a).

(2) Calculation of yarn axis helix angle δ_0, by Equations (2–55), (2–32) and (2–56) or (2–56a) or (2–56b) or (2–56c).

Table 4.2 Numerical example to determine the stress-strain curve of 2-ply cord 2-yarn strand of 1.67 mm diameter, 138 turns per m upper twist (Z), 276 turns per m lower twist (S) and $\alpha_0=14.2°$.

λ_t	λ_i	λ_p	λ_c	σ_i (gr/den)	σ_p (gr/den)	σ_c (gr/den)
1.00	1.00	1.00	1.00	0.00	0.00	0.00
1.02	1.02	1.02	1.02	0.43	0.39	0.35
1.04	1.04	1.04	1.05	0.69	0.62	0.55
1.06	1.06	1.06	1.08	0.90	0.80	0.72
1.08	1.08	1.08	1.10	1.10	0.96	0.86
1.10	1.10	1.11	1.13	1.35	1.16	1.05
1.12	1.12	1.13	1.15	1.63	1.38	1.24
1.14	1.14	1.15	1.17	1.96	1.63	1.48
1.16	1.16	1.17	1.20	2.36	1.94	1.75
1.18	1.18	1.19	1.22	2.75	2.22	2.01
1.20	1.20	1.21	1.25	3.30	2.62	2.39
1.22	1.21	1.23	1.27	3.74	2.93	2.67
1.24	1.23	1.25	1.29	4.13	3.18	2.90
1.26	1.25	1.27	1.32	4.50	3.42	3.12
1.28	1.27	1.29	1.34	4.83	3.62	3.31

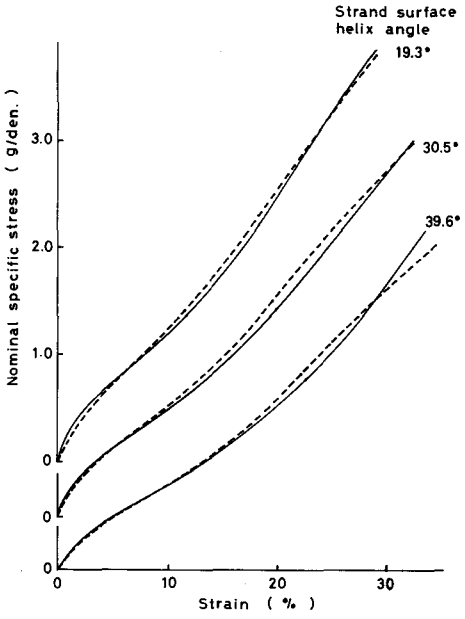

Fig. 4.8. Calculated and experimental stress-strain curves of 2-yarn strand at various degrees of twisting.
solid line; experimental, broken line; calculated

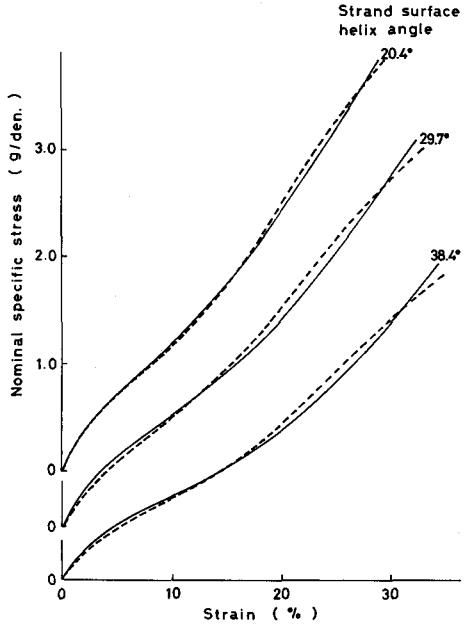

Fig. 4.9. Calculated and experimental stress-strain curves of 3-yarn strand at various degrees of twisting.
solid line; experimental, broken line; calculated.

(3) Calculation of yarn surface helix angle in the outer ply in the strand by using Equations (2–57) and (2–58).
(4) Calculation of fibril helix angle at neutral zone layer α_0 from the obtained β_0, using Equation (2–1).

Then, the derivation of cord stress-strain curve from the initial yarn stress-strain curve can be done as follows (See Fig. 4.7).

(5)— (6) Determination of λ_i from the given λ_f and the obtained α_0, using Equation (2–5).
(6)— (7) Determination of σ_i from the initial yarn stress-strain curve.
(7)— (8) Determination of σ_f from σ_i using Equation (2–18)
(5)— (9) Determination of λ_p from λ_i using Equation (2–59).
(8)—(10) Determination of σ_p from σ_i using Equation (2–72).
(9)—(11) Determination of λ_c from λ_p using Equation (2–60).
(10)—(12) Determination of σ_c from σ_p using Equation (2–73).

The stress-strain curve of twisted monofilament as ply in the strand and the stress-strain curve of the strand is not drawn. As an example numerical calculation for 2–ply cord 2-yarn strand stress-strain relationship is given in Table 4.2. The results of the stress-strain curve calculation for the strand and cord of multiply-

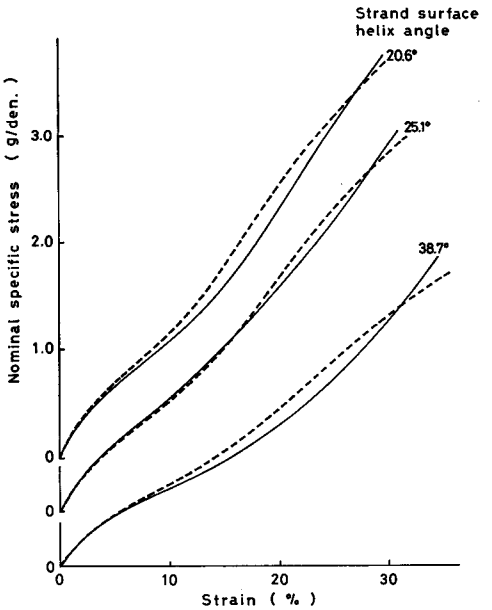

Fig. 4.10. Calculated and experimental stress-strain curves of 7-yarn strand at various degrees of twisting.
solid line; experimental, broken line; calculated.

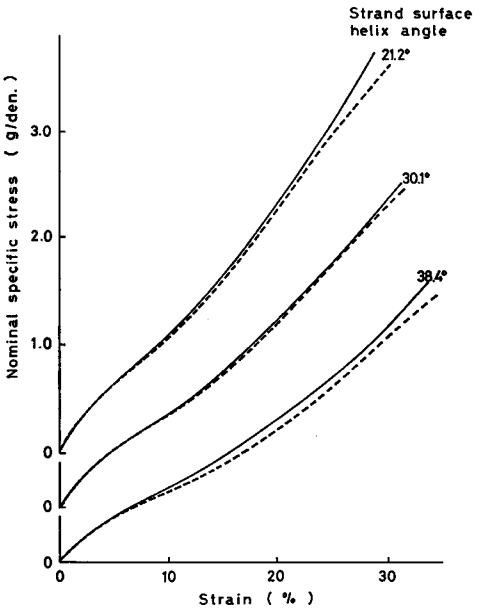

Fig. 4.11. Calculated and experimental stress-strain curves of 19-yarn strand at various degrees of twisting.
solid line; experimental, broken line; calculated.

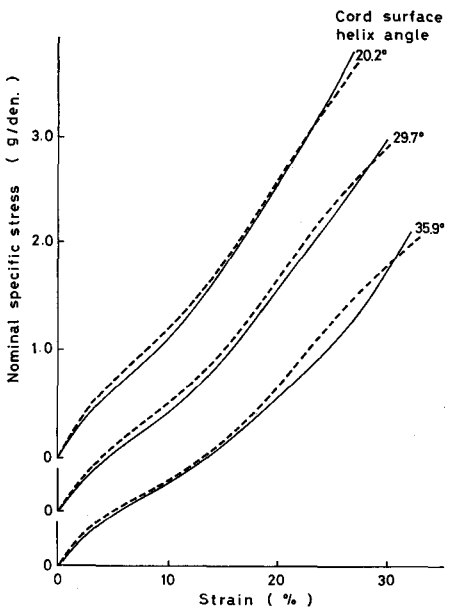

Fig. 4.12. Calculated and experimental stress-strain curves of 2-ply cord 2-yarn strand at various degrees of twisting. solid line; experimental, broken line; calculated.

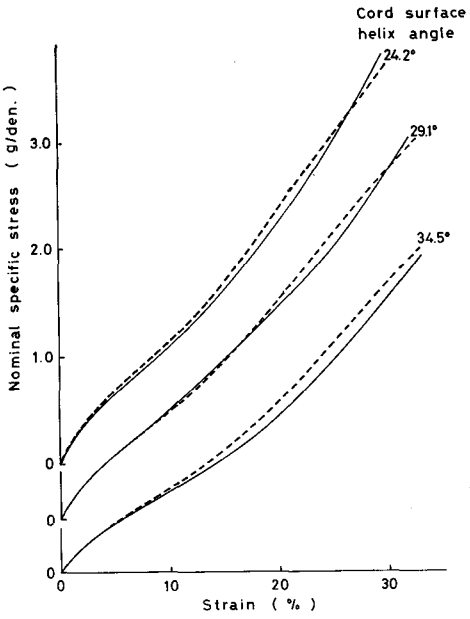

Fig. 4.13. Calculated and experimental stress-strain curves of 2-ply cord 3-yarn strand at various degrees of twisting. solid line; experimental, broken line; calculated.

yarn strand shows a close agreement with the experimental curve, although some deviations still exist. In general the cord and strand theoretical curves deviate to the larger values of stress from its corresponding experimental curve at the same condition of strain, except for the strand of 19-ply yarns. This is may be due to the calculation which refered only to the yarn at the outer ply. Representative figures are given below (Fig. 4.8–Fig. 4.19).

5. Discussion

A theoretical calculation was developed to calculate the stress-strain curve of cord from the initial monofilament yarn stress-strain curve. Experiments applying two kinds of samples of cords with single-yarn strand and with multiply-yarn strand were carried out to compare the results with the calculated values.

The calculation of strain is based on the geometrical methods similar to those used by Treloar, L.R.G and G. Ridging in their papers[15,16]. The stresses were calculated on the basis of usual method by calculating the ratio of force to the cross sectional area. In this study the stresses were represented as the nominal specific stress defined as a ratio of the force to the mass/unit length. This is a more

convenient quantity than the conventional stress in terms of force/unit area for textile applications. Treloar and Riding[15,16] analyze the stresses using the strain-energy method.

In developing the theoretical calculation, basic and additional assumptions were adopted, and since the assumptions may not correspond precisely with the actual situations, these assumption will however bring some deviations to the calculated values from experimental results. On the other hand without adopting the assumptions it would be very difficult to arrive at a theoretical solution. The validity of these assumptions has, however, been investigated by the actual observations and measurements. The assumption of constancy of volume during deformation has been justified as to be sufficiently true for all textile filaments, especially for large strains[12]. In this study this validity of constant volume assumption was investigated by observing the diameter change during tensioning of a Nylon monofilament yarn No. 150. The results of this observation is that the assumption may be considered to be true for this study. (see Fig. 5.1)

The adoption of the Treloar's theory[15] for the calculation of the stress value merely without any modification gives a large deviation in the theoretical curve compared with experimental result. An example of the theoretical curve calculated using Treloar's formulae shows the deviation of a larger value of stress from the

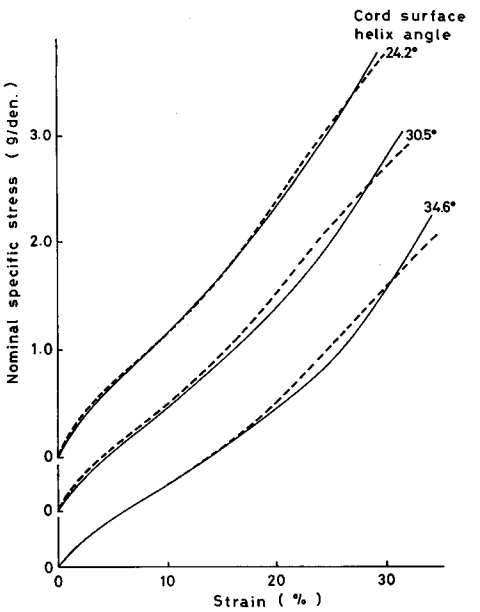

Fig. 4.14. Calculated and experimental stress-strain curves of 3-ply cord 2-yarn strand at various degrees of twisting. solid line; experimental, broken line; calculated.

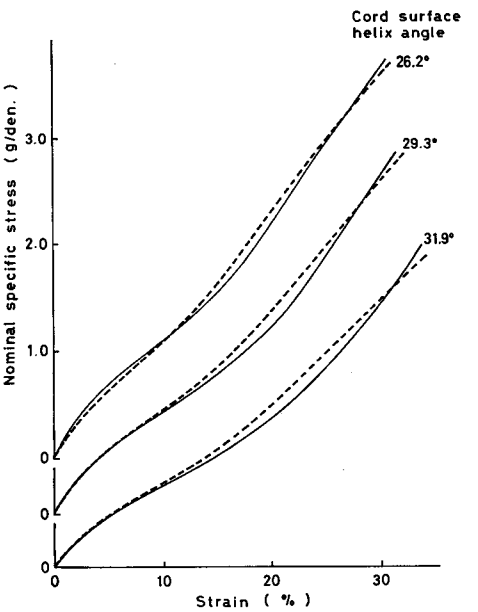

Fig. 4.15. Calculated and experimental stress-strain curves of 3-ply cord 3-yarn strand at various degrees of twisting. solid line; experimental, broken line; calculated.

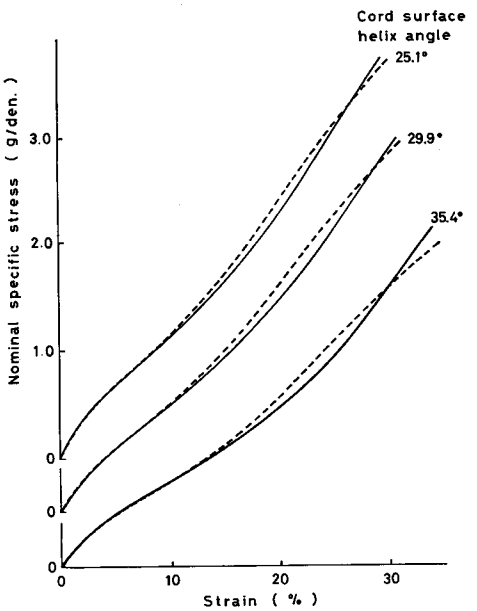

Fig. 4.16. Calculated and experimental stress-strain curves of 2-ply cord 7-yarn strand at various degrees of twisting. solid line; experimental, broken line; calculated.

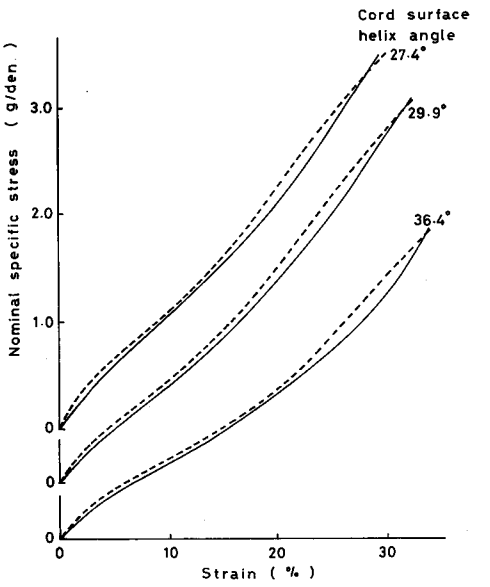

Fig. 4.17. Calculated and experimental stress-strain curves of 3-ply cord 7-yarn strand at various degrees of twisting. solid line; experimental, broken line; calculated.

experimental curve at the same condition of strain (see Fig. 5.2). The theoretical curve calculated in this study shows a close agreement although some deviations still exist, in this case the theoretical curve deviates to a larger value of stress compare with the experimental curve for the same condition of strain, but the deviation shown by the calculated curve of this study is only slight. In general, this study gives a much better agreement than that using Treloar's formulae. However, in comparing this theory, the behaviour of the different materials, the difference prcoedures in sample preparation and the different descriptions of cord as its final product (which have a noticeable influence on the properties of the system) still have to be considered.

Anyway, it is shown in this study that the prediction of the stress-strain curve of a cord from the initial yarn stress-strain curve can be realized. For the further purposes of designing netting materials, it may be possible to determine the construction of a cord with a desired form of stress-strain curve.

From the comparison between the calculated and experimental stress-strain curves it can be seen that the agreement between calculated and experimental curves is sufficiently good both for cords of single yarn strand and of multiply-yarn strand, although some deviations still have been found. These deviations are probably caused by the following reasons.

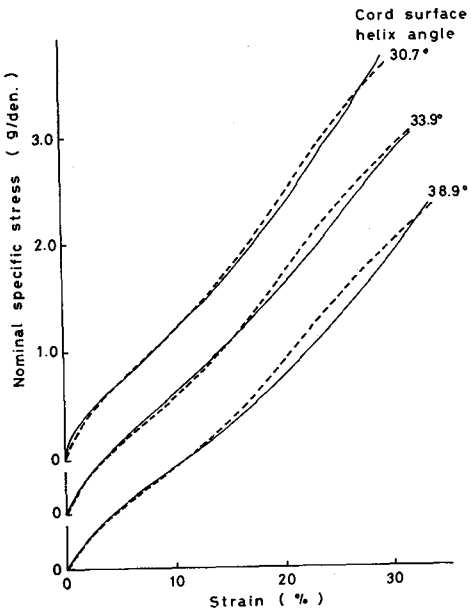

Fig. 4.18. Calculated and experimental stress-strain curves of 2-ply cord 19-yarn strand at various degrees of twisting.
solid line; experimental, broken line; calculated.

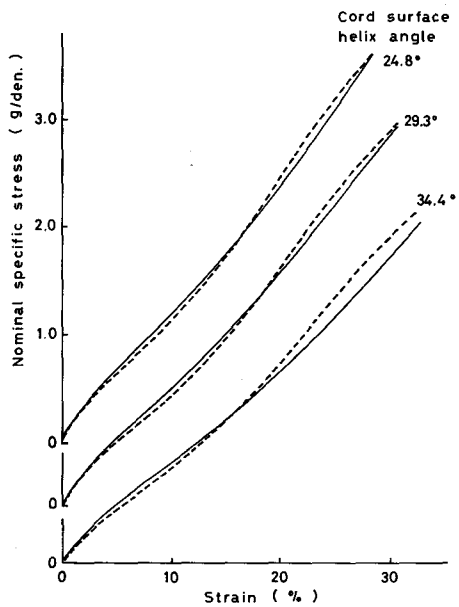

Fig. 4.19. Calculated and experimental stress-strain curves of 3-ply cord 19-yarn strand at various degrees of twisting.
solid line; experimental, broken line; calculated

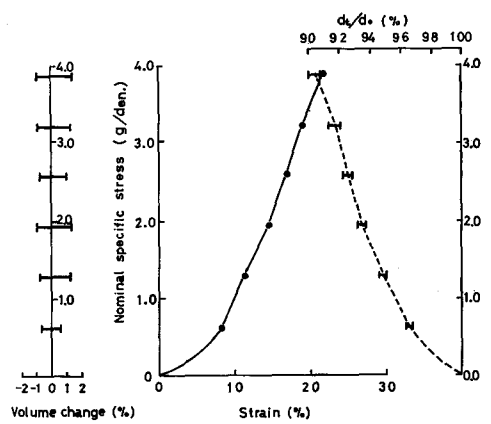

Fig. 5.1. Monofilament yarn diameter and volume change by tension.

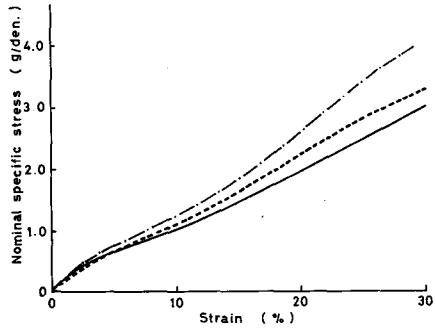

Fig. 5.2. Comparison between calculated curve of the present study and calculated using Treloar's formula with experimental result for 3-ply cord single yarn strand at 40.9° surface helix angle.
——; experimental curve, -·-·-; calculated using Treloar's formula,
----; calculated in present paper.

(1) The assumption that the modulus of elasticity of the fibril in the monofilament is constant throughout compressing and tensioning has been used in deriving the theoretical calculation for the tensile properties of twisted monofilament yarn. This, may not correspond precisely with the experimental situation which is in general, continuously changable through deformation, for textile materials.

(2). The assumption that the shape of the ply sections remained circular without any distortion during deformation, does not seem to be true. The observations on the cross sections of cords show that the individual yarns in the ply move closer to each other as twisting increases, and that the air space decreases because of the closer packing of the yarns in the high twists. Under the tension, it can be seen that the monofilament yarn becomes more compact, the air space disappeared and the individual monofilament yarn cross sections became irregular and could not maintain their circular forms. This will result in a decrease in the diameter of cords from that of calculated values obtained based on this assumption. These phenomena were shown by the results of the experiments described in Chapter 3 section 3.2.2 about the observation on the cord cross section and the cord diameter change by tension. In comparing the results of these experiments with the corresponding calculated values, the experimental values indicate a more considerable decrease by tensional force.

(3). The effect of transverse force. The changes in the cross sections of ply and cord and of the individual monofilament yarn are thought to be caused by the transverse force which resulted in a lateral pressure between monofilament yarns in which are not taken into account in this study. The problem of transverse forces were studied by Hearle, J.W.S.[11], Batra, S.K.[35,36] and Wilson, N.[37]. In Heale's paper it was stated that the fibres at the centre of a yarn will be under a considerable transverse compressive force and that this may affect the breaking extension of yarn with twists. Batra, S.K. in his paper wrote that in the particular

core where the helix angle remain constant, it is realized that the lateral pressure depends not only on tension in the fibre but also on the shear force, which in turn, depends on the bending and torsional rigidities. Wilson, N. in his paper wrote that on the twisting of yarns, transverse force on the filaments decreases the stress in them for a given strain and also distorts their circular cross sections. The quantity of the lateral stress depends on the average inward pressure on a filament due to every filaments in the yarn. These inward pressures will be the greatest for the filament in the center, less for the inner layer filaments and for the outer filaments this inward pressures will be zero. Batra, S.K. gave the indication that these pressures decreased from the centre filament to the outer layer filaments by numerical values[36]. From these views, if the effect of lateral forces are regarded, it seems that it was in fact better to calculate the stress in the cord from the corresponding stress in the outer layer yarn, as done in this study, since this yarn in the outer ply endure the least lateral pressure. Ogata, N. and K. Yoshida[38] also made a study on the lateral force by investigating the withdrawal force of a tape inserted between two filaments which show that the lateral force in the yarn is only dependent on its tension, but it was difficult to estimate the absolute value of the lateral force by this method.

The other factor in the transverse force is the friction between filaments, but comparatively little published work is available. Guthrie, J.C. and P.H. Oliver[39] wrote about the importance of the frictional force of textile fibres in the textile processing. Postle, L.J. et al.[40] described the investigating of the inter fibre frictional force in wool and slivers. No publication on the effect of the frictional force in the stress-strain properties of yarn and cord has been found.

(4) Problem of migration. The problem of migration is known in the practice as the deviation from the idealized çylindrical structure. In the actual yarn the migration occurs as a result of the acting of filaments naturally trying to become the same length during construction of the yarn. But according to Treloar, L.R.G.[41,42], the effect of migration on the geometrical and tensile properties of yarn is generally slight, and would be non significant even for the most extreme values of the migration parameter. His conclusion provides a justification for the general use of simple coaxial helix theory even though migration on filament is known to be present.

6. Conclusions

From the results given, it is seen that, for the cords of single-yarn strand and of multiply-yarn strand, the theory presented in Chapter 2 does predict qualitatively well the stress-strain curve derived from the stress strain curve of the initial monofilament yarn.

The fact that for highly twist of cords the experimental values of cord stress are low relative to the calculated values are probably due to the assumptions that were adopted such as the constancy of fibril elasticity modulus in deformation, disregarding of the transverse forces, the constancy of ply cross sectional shape during deformation and hence the disregarding of the packing density problem.

These will factors caused the deviations in the calculated values from the corresponding results. However, complete verification of a more exact theory is still difficult because of the inherent variability of textile materials.

Finally as the result of this study for the purpose of designing netting materials from the known stress-strain curve of an initial yarn, the configuration of a cord with a certain desired form of stress-strain curve within a reasonable range may be constructed.

References

1. Finn, D.B. 1959. Preface. *Modern Fishing Gear of the World.* XXIII.
2. Arzano, R. 1959. Man-made fibres. *Modern Fishing Gear of the World.* 13–18.
3. Treloar, L.R.G. 1956. The geometry of multi-ply yarns. *J. Text. Inst.*, **47**, T348–T368.
4. Gracie, P.S. 1960. Twist geometry and twist limits in yarns and cords. *J. Text. Inst.*, **51**, T271–T288.
5. Freeston, W.D., Jr. and M.M. Schoppee. 1975. Geometry of bent continuous-filament yanrs. *Text. Res. J.*, **45**, 835–852.
6. Riding, G. 1962. A simplified method of making core yarns. *J. Text. Inst.*, **53**, P117–P185.
7. Tattersall, G.H. 1958. An experimental study of yarn geometry. *J. Text. Inst.*, **48**, T295–T304.
8. Riding, G. 1961. A study of the geometrical structure of multi-ply yarns. *J. Text. Inst.*, **52**, T366–T381.
9. Iyer, K.B. 1965. Some aspects of yarn structure. *J. Text. Inst.*, **56**, T225–T247.
10. Hearle, J.W.S. and O.N. Bose. 1966. The form of yarn twisting. *J. Text. Inst.*, **57**, T294–T320.
11. Hearle, J.W.S. 1958. The mechanics of twisted yarns: The influence of transverse forces on tensile behaviour. *J. Text. Inst.*, **49**, T398–T408.
12. Treloar, L.R.G. and G. Riding. 1963. A theory of the stress-strain properties of continuous-filament yarns. *J. Text. Inst.*, **54**, T156–T270.
13. Kilby, W.F. 1964. The mechanical properties of twisted continuous-filament yearns. *J. Text. Inst.*, **55**, T589–T632.
14. Platt, M.M. 1950. Mechanics of elastic performance of textile materials. *Text. Res. J.*, **20**, 1–15.
15. Treloar, L.R.G. 1965. The stress-strain properties of multi-ply cords. Part I. Theory. *J. Text. Inst.*, **56**, T477–T488.
16. Riding, G. 1965. The stress-strain properties of multi-ply cords. Part II. Experimental. *J. Text. Inst.*, **56**, T489–T497.
17. Tauti, M. 1929. Studies of netting cords IV. Strength of cord in relation to the twist. *J. of the Imperial Fisheries Inst.*, **25**, 27–40.
18. Koizumi, T. 1953. The tensile strength of Saran netting cord of various twist. *Bull. Jap. Soc. Sci.*, **20**, 569.
19. Koizumi, T. 1955. The tensile strength of Kurehalon netting cord of various twist. *Bull. Jap. Soc. Sci.*, **20**, 759–759.
20. Koizumi, T. 1955. The tensile strength of Amilan net netting cords of various twist. *Bull. Jap. Soc. Sci.*, **21**, 139–141.
21. Honda, K. and S. Osada. 1964. Polypropylene in Japan. *Modern Fishing Gear of the World* 2, 55–56.
22. Shimozaki, Y. and H. Kato. 1959. On the wear resistance in continuous filament-twines-I. *Bull. Jap. Soc. Sci.*, **24**, 787–794.

23. Sato, O. et. al. 1974. Change of breaking tensile strength of thread by bending (I) Thread of monofilafilament. *Bull. Fac. Fish., Hokkaido Univ.*, **24**, 171–178.
24. Yamamoto, K. 1980. Fundamental studies on the geometrical and the mechanical properties of netting twines. Doctor Thesis (unpublished), Faculty of Fisheries, Hokkaido Univ.
25. Annonymous. 1960. Standardisation. *J. Text. Inst.*, **51**, p 87.
26. Hayhurst, G.A. and A. Robinson. 1959. Construction and numbering of synthethic net twines. *Modern Fishing Gear of the World.* 4–5.
27. Stutz, H. 1959. Termonology and count of synthethic fibre twines for fishing purposes. *Modern Fishing Gear of the World.* 1–3.
28. Takayama, S. 1959. Terminology and numbering systems used in Japan. *Modern Fishing Gear of the World*, 6–7.
29. Klust, G. 1964. Standardisation of terminology and numbering systems for netting twines. *Modern Fishing Gear of the World.* 2, 3–8.
30. Robinson, A. 1964. Discussion. Standardisation of terminology and numbering systems for netting twines. *Modern Fishing Gear of the World.* 2, 8.
31. Zurek, W. et. al. 1976. Elastic properties of twisted monofilaments. *Text. Res. J.*, **46**, 381–393.
32. Murdiyanto, B. and O. Sato. 1978. Studies on the breaking mechanism of continuous multifilaments I. On the stress-strain properties of twisted monofilaments. *Bull. Fac. Fish., Hokkaido Univ.*, **29**, 349–362.
33. Love, A.E.H. 1927. Mathematical theory of elasticity. *Cambridge. Chapter* 8, 381–398.
34. Yamamoto, K. 1978. Twist geometry on strand and 3-ply Cord – I. On the cross-sectional form of ply in the cord and cording limit. *Bull. Jap. Soc. Sci.*, **44**, 1213–1216.
35. Batra, S.K. 1973. The normal force between twisted filaments, Part I: The fibre-wound-on-cylinder model analytical treatment. *J. Text. Inst.*, **64**, 209–222.
36. Batra, S.K. et. al. 1973. The normal forces between twisted filaments, Part II: Experimental verification. *J. Text. Inst.*, **64**, 363–373.
37. Wilson, N. 1962. Rubber models of yarns and cords: The twisting of multi-filament models. *J. Appl. Phys.*, **13**, 323–330.
38. Ogata, N. and K. Yoshida. 1978. Change of lateral force in Nylon–6 yarns. *Text. Res. J.*, **48**, 542–547.
39. Guthrie, J.C. and P.H. Oliver. 1952. Inter-fibre friction of viscose Rayon. *J. Text. Inst.*, **43**, T579–T594.
40. Postle, L.J. and J. Ingham. 1952. The measurement of inter-fibre friction in slivers. *J. Text. Inst.*, **43**, T77–T90.
41. Treloar, L.R.G. 1965. A migrating-filament theory of yarn properties. *J. Text. Inst.*, **56**, T359–T380.
42. Treloar, L.R.G. and G. Riding. 1965. Migrating-filament theory: Apparent variation of twist with radial position. *J. Text. Inst.*, **56**, T381–T388.

Appendix

The solution Equation (2–9) is given as follows

$$F_t = 2\pi E \int_0^{R_t} \left\{ \frac{\sec \theta_t}{\sec \alpha_t} (\varepsilon_{t(\alpha)} + 1) - 1 \right\} r_t \cos^2 \theta_t dr_t$$

$$F_t = 2\pi E \int_0^{R_t} \left(\frac{\sec \theta_t}{\sec \alpha_t} \cdot \varepsilon_{t(\alpha)} \right) \cos^2 \theta_t r_t dr_t$$

$$+ 2\pi E \int_0^{R_t} \left(\frac{\sec \theta_t}{\sec \alpha_t} - 1 \right) \cos^2 \theta_t r_t dr_t \tag{1}$$

By the reason of the proportionality with Equation (11) in the previous paper[32], the value of

$$2\pi E \int_0^{R_t} \left(\frac{\sec \theta_t}{\sec \alpha_t} - 1 \right) \cos^2 \theta_t r_t dr_t = 0 \tag{2}$$

Then

$$F_t = 2\pi E \int_0^{R_t} \left(\frac{\sec \theta_t}{\sec \alpha_t} \varepsilon_{t(\alpha)} \right) \cos^2 \theta_t r_t dr_t$$

$$= \frac{2\pi E \varepsilon_{t(\alpha)}}{\sec \alpha_t} \int_0^{R_t} \cos \theta_t r_t dr_t \tag{3}$$

Let us considered that

$$\tan \theta = \frac{2\pi r}{h} \tag{4}$$

or,

$$r = \frac{h}{2\pi} \tan \theta \tag{5}$$

and then

$$dr = \frac{h}{2\pi} d(\tan \theta) \tag{6}$$

Hence,

$$r\,dr = \left(\frac{h}{2\pi} \right)^2 \tan \theta d(\tan \theta)$$

$$= \left(\frac{h}{2\pi} \right)^2 \tan \theta \sec^2 \theta\, d\theta \tag{7}$$

Substitution of Equation (7) into (3) regarding the subscript t, results

$$F_t = \frac{2\pi E\varepsilon_{t(\alpha)}}{\sec \alpha_t} \int_0^{\beta_t} \cos \theta_t \tan \theta_t \sec^2 \theta_t \left(\frac{h}{2\pi}\right)^2 d\theta_t$$

$$= \frac{2\pi E\varepsilon_{t(\alpha)}}{\sec \alpha_t} \left(\frac{h}{2\pi}\right)^2 \int_0^{\beta_t} \tan \theta_t \sec \theta_t d\theta_t \tag{8}$$

Hence,

$$F_t = \frac{2\pi E\varepsilon_{t(\alpha)}}{\sec \alpha_t} \left(\frac{h_t}{2\pi}\right)^2 [\sec \theta_t]_0^{\beta_t}$$

$$= \frac{2\pi E\varepsilon_{t(\alpha)}}{\sec \alpha_t} \left(\frac{h_t}{2\pi}\right)^2 (\sec \beta_t - 1) \tag{9}$$

With the proportionality of α and β during tensioning, then

$$\frac{r_{0(\alpha)}}{R_0} = \frac{r_{t(\alpha)}}{R_t} = \frac{\tan \alpha_0}{\tan \beta_0} = \frac{\tan \alpha_t}{\tan \beta_t} \tag{10}$$

and

$$\tan^2 \alpha_t = \frac{\tan^2 \alpha_0}{\tan^2 \beta_0} \tan^2 \beta_t \tag{11}$$

or it can be written

$$\sec^2 \alpha_t = \frac{(\sec^2 \alpha_0 - 1)}{\tan^2 \beta_0} \tan^2 \beta_t + 1 \tag{12}$$

According to Equation (2–1) and (2–13), then

$$\sec^2 \alpha_t = \frac{\left(\frac{\sec \beta_0 - 1}{ln \sec \beta_0}\right)^2 - 1}{\tan^2 \beta_0} \lambda_t^{-3} \tan^2 \beta_0 + 1$$

$$= 1 + \lambda_t^{-3} \left\{ \left(\frac{\sec \beta_0 - 1}{ln \sec \beta_0}\right)^2 - 1 \right\} \tag{13}$$

or

$$\sec \alpha_t = \left[1 + \lambda_t^{-3} \left\{ \left(\frac{\sec \beta_0 - 1}{ln \sec \beta_0}\right)^2 - 1 \right\} \right]^{1/2} \tag{14}$$

Substitution of (14) into (9) results

$$F_t = \frac{E\varepsilon_{t(\alpha)} h_t^2 2(\sec \beta_t - 1)}{4\pi \left[1 + \lambda_t^{-3} \left\{ \left(\frac{\sec \beta_0 - 1}{ln \sec \beta_0}\right)^2 - 1 \right\} \right]^{1/2}} \tag{15}$$

This is the Equation (2–10) in the text.